Effect of magnesium addition on the cell structure of foams produced from re-melted aluminium alloy scrap

G. S. Vinod-Kumar[1,4*], K. Heim[1,2], J. Jerry[4], F. Garcia-Moreno[1,2],A. R. Kennedy[3], J. Banhart[1,2]

[1]Technische Universität Berlin, Hardenbergstraße 36, 10623 Berlin, Germany

[2]Helmholtz-Zentrum Berlin für Materialien und Energie, Hahn Meitner Platz, 14109 Berlin, Germany

[3]Division of Manufacturing, University of Nottingham, Nottingham, NG2 7RD, UK,

[4] SRM Research Institute, SRM University, Kattankulathur, 603203, India

Abstract

Closed cell foams were produced from re-melted aluminium alloy scrap that contained 0.13 wt.% Mg magnesium in the as-received state and higher levels after adding 1, 2 or 5 wt.% Mg. The excess Mg gave rise to the fragmentation of long oxide filaments present in the scrap alloy into smaller filaments and improved its distribution and wetting by the Al matrix. Foaming the re-melted scrap alloy containing 1,2 and 5 wt.% Mg excess showed stability and good expansion in comparison to the scrap alloy containing 0.13 wt.% Mg only, but the cell became non-equiaxed when the Mg concentration was high (≥2 wt.% excess) due to cell wall rupture during solidification. The compressibility and energy absorption behaviour was studied for scrap alloy foams containing 1 wt.% Mg excess, which is the optimum level to obtain good expansion, stability and uniform cell size. Foams with densities in the range of 0.2-0.4 $g.cm^{-1}$produced by holding at the foaming temperature for different times were used for the investigation. A uniform cell structure led to flatter stress plateaus, higher energy absorption efficiencies and reduced "knockdown" in strength compared with commercial foams made by gas bubbling. The mechanical performance found is comparable to that of commercial foams made by a similar method but the expected costs are lower.

* Corresponding Author: Dr. G. S. Vinod Kumar, email id: vinodnarasimha@gmail.com

Keywords

Scrap aluminium alloy, Closed cell Al foams, oxide bi-films, $MgAl_2O_4$ (spinal), compressive strength

1. Introduction

Closed-cell aluminum alloy foams produced through the liquid metal route are potentially cheaper in comparison to foams produced using metal powders because of the lower number of processing steps [1-2]. Liquid metal foaming requires ceramic or intermetallic particles for foam stabilization [3-5].Ceramic particles such as SiC, Al_2O_3, TiB_2, TiC [6] and also $MgAl_2O_4$[7] have been found to be effective stabilizing agents for aluminum foams but the introduction of these particles into the matrix requires additional processing steps. There is a school of thought that oxide bi-films which get entrapped during ingot casting will also acts as stabilization agent for foams[6, 8].

Attempts have been made to utilise the foam-stabilizing properties of oxide bi-films by using scrap aluminium alloys produced by melting swarfs (machining chips and turnings of automotive castings) as a foamable precursor. By re-melting these swarfs the thick oxide skins contained are introduced into the alloy as oxide films. Ha et al. reported that these oxide films enhance viscosity of the melt and aid in foaming [9]. Haesche et al. have utilised thixocasting to produce foamable precursors from AlSi9Cu3 or AlMg4.5Mn alloy chips and $CaCO_3$ or $CaMg(CO_3)_2$ as a blowing agent[10]. However, in all previous studies it was reported that the observed cell morphology of scrap aluminium alloy foam was distorted due to the poor distribution of inherent oxides in the matrix. Using scrap alloys for foaming finds potential due to its low cost in comparison to expensive particle-reinforced metal matrix composites produced by ex-situ or in-situ methods. The authors in their previous studies[11-12] have demonstrated that re-melted scrap aluminium alloy foams with optimum expansion and stability can be made by adding Mg while melting the swarfs(machining chips or turnings of

LM26 alloy castings) and holding them in the liquid state during which the oxides are dispersed. To enable the reaction, the oxide concentration in the scrap was increased by heat treating the swarfs at 500^{o}C for several hours before melting. 1 or 2 wt.% Mg was added and this Mg reacts with the oxides to form $MgAl_2O_4$ (spinel) and MgO as reaction products. This promotes good wetting of oxides and distributes them uniformly in the Al matrix.

In the work presented here, the cell structure and cell size distribution of re-melted Al scrap alloy foams containing various concentrations of Mg (0.13 wt.% as-received, and 1, 2 and 5 wt.% in excess to this level) and foamed at various holding time was investigated. The aim of this study was to understand to which extent the inherent oxides filaments undergo fragmentation and how much $MgAl_2O_4$ and MgO is formed when Mg is added at increased levels. The results are correlated to the expansion, stability, cell structure and cell size distribution of the foams produced. The main difference between the scrap alloy used in the present and previous work [11-12] is the oxide concentration, which is less in the present work since no heat treatment was carried out for the swarfs before melting.

The prospects of using re-melted Al scrap alloy foams in structural applications have to be evaluated even though they show a promising foaming behaviour. The base alloy of the swarfs, LM26, exhibits very low ductility and the presence of oxides further decreases ductility and deteriorates the mechanical properties of the foam. Therefore, the compressibility and the energy absorption behaviour of foams of various densities displaying good cell structure and distribution were studied. Their performance is compared to foams made by commercially available liquid routes, also known as Cymat and Alporas foams.

2. Experimental Procedure

The scrap used in the present study was received as mm-sized swarfs (machining chips and turnings) of LM26 (Al–10 wt.%Si–3 wt.% Cu) alloy, which is commonly used for making automotive castings. The morphology of the chips and the approximate composition as meas-

ured by optical emission spectroscopy (OES) has been reported in Ref.[11].The machining chips already contain 0.13 wt.% of Mg in the as-received state. The material was first heated to 673 K (400 °C) to remove residual oil and cutting lubricants. Then it was directly converted into ingots by melting in a graphite crucible at 1023 K (750 ºC). No additional heat treatment was carried out as done in previous studies where the oxide content in the swarfs was increased [11-12].During melting, the chips were fused by vigorous intermittent stirring for 30 min. Magnesium was admixed in excess to 0.13 wt.% (base alloy concentration) at various levels (1, 2 and 5 wt.%) by using a Al-25 wt.% Mg master alloy. After this, the melt was kept isothermally at 1023 K (750 ºC) for 4 h for conditioning (reaction). The conditioned melt was again stirred and cast into a steel mould. X-ray diffraction for phase analysis of the scrap alloys was performed using Cu-K_α radiation. The re-melted scrap alloys (and cross sections of foams) were metallographically polished and electro-polished using a mixture of orthophosphoric acid, ethanol and water as the electrolyte. The polished samples were observed using a high-resolution scanning electron microscope (HRSEM). Elemental analysis was done using energy dispersive X-ray spectroscopy (EDX).

Foaming was performed by melting 40 g of each alloy in an alumina crucible in a resistive heating furnace at 973 K (700 ºC). After the melt had reached the desired temperature, 1.6 wt.% of as-received TiH_2 powder was admixed to the melt using a graphite stirrer rotating at 600 rpm for 80 s. After mixing, the melt was held isothermally inside the furnace for different holding times, namely100 s, 140 s and 180 s, during which it was allowed to foam, after which the sample was taken out and allowed to solidify in resting air. X-ray tomography of the foams was performed by rotating them through 360° in steps of 1° while acquiring X-ray radiographic images after each step. Three-dimensional (3D) reconstruction of the data was carried out using the commercial software 'Octopus'. After reconstruction, the commercial software 'VGStudioMax 1.2.1' was used to extract 2D and 3D sections of the foam. The 2D cell area dis-

99 tribution and circularity for selected foams was calculated by analyzing the reconstructed tomo-
100 graphic slices taken from the central part of the foams. This analysis was performed by using the
101 software 'ImageJ 1.35j'.

102 For compression tests, foams were made from alloy containing a Mg excess of 1 wt.% and
103 applying holding times of either 100 s or 140 s. Samples of~(25×25×25) mm^3size were sliced
104 by electro-discharge machining. The resulting specimens had various densities as given in
105 Table 1. Compression testing was performed at a rate of 2 $mm \cdot min^{-1}$. Mechanical testing and
106 data analysis were conducted according to "ISO 13314:2011(E)" standard.

107

108 **3 Results**

109 Figures 1a and b show SEM photomicrographs of re-melted scrap alloy in the as-received
110 condition (containing 0.13wt.% of Mg) and in the alloy with 1wt.% excess Mg addition. The
111 longer aluminium oxide filaments seen in the aluminium matrix (Fig. 1a) containing only
112 0.13 wt.% of Mg get fragmented into smaller oxide films after adding 1 wt.%
113 Mg(Fig. 1b).The alloy also shows Fe- and Cu-based intermetallic compounds in the matrix. A
114 closer look at the microstructure (Fig.1c&d) of the re-melted scrap alloy containing 1wt.%
115 Mg shows that the surface of the fragmented oxide films is covered by fine $MgAl_2O_4$ (spinel)
116 particles of less than 2 μm size. The EDX spectrums stacked (Fig.1e) taken at different parti-
117 cles (one spectrum for each particle) confirms the presence of Al_2O_3, $MgAl_2O_4$ and other Fe-
118 and Cu-based intermetallic compounds in the aluminium matrix.

119 The X-ray diffraction patterns (Fig. 2) of the re-melted aluminium scrap alloys containing
120 various amounts of Mg (0, 1, 2 and 5 wt.% in excess to the 0.13 wt.% in the as-received ma-
121 terial) point at the presence of $MgAl_2O_4$, MgO, Mg_2Si and small amounts of other transition
122 phases. The XRD spectra show that addition of more Mg does not increase the amount of

$MgAl_2O_4$ or MgO in the alloys as seen by the peak intensities of the spectra. Their formation is rather governed by the amount of oxygen available in an alloy, which is independent of Mg content. However, increasing the Mg content does increase the level of Mg_2Si formation.

Figure 3 a-b shows X-ray tomographic reconstructions of longitudinal cross sections of foams produced from re-melted scrap alloys containing 0.13 wt.% Mg. The foams were produced at 973 K (700 °C) and held for 100 s (Fig.3a) or 140 s (Fig.3b) and were solidified by air cooling. The foam showed good expansion after 100 s of holding at the foaming temperature and its macrostructure exhibits an equiaxed cell structure and uniform cell size distribution throughout the cross section. No defects such cell wall rupture, deformed cells or drainage are observed. Upon holding for 140 s the foam started to collapse. The liquid sump at the bottom of the foam indicates drainage (Fig. 3b).The 2-Dcell size distribution of the foam obtained after 100 s of holding is given in Fig. 3c. The analysis is based on the area fraction, which is defined as the area contribution of a cell size class related to the total area of all the cells [13].The mean cell size D as provided by log-normal fitting of the distributions is 3.42±0.1 mm. The cells in the foam held for 140 s are full of defects and irregular and therefore no reliable analysis could be performed.

The 2D cell circularity of the foam obtained after 100 s of holding shows (Fig. 3d) that most of the cells are close to circularity, indicating that they are of equiaxed (polyhedral) shape. Here, the circularity C of a cell is defined as $4\pi A/P^2$, where A and P are the area and perimeter of the cell, respectively. If C approaches 1, a cell resembles a circle. The details of the analysis are reported in Ref. [13].

Figure 4 a-c shows 3D X-ray tomographic reconstructions of longitudinal cross sections of foams produced from re-melted scrap alloys containing 1, 2 and 5 wt.% Mg addition. The foams were produced at 973 K (700 °C) and held for 140 s before solidification. Figure 4 d shows the macrostructure of the foam containing 5 wt.% Mg, which was held for 180 s. For

100 s holding time, the expansion was not complete for the foams containing 1, 2 and 5 wt.% Mg addition. Delayed expansion of foam with increased Mg content was already reported in Refs. [11-12]. The foam with 1 wt.% Mg addition showed good expansion and stability even after 140 s of holding unlike the foam with 0.13 wt.% Mg content. The cells are finer and equiaxed in shape and uniformly distributed throughout the cross section. The expansion observed for the foams with 2 and 5 wt.% Mg is less in comparison to that of the foam containing 1 wt.% Mg. The cell structure of the foams with 2 and 5 wt.% Mg addition are non-equiaxed in shape in comparison to 1 wt.% Mg, see below for a quantitative analysis. To witness expansion during further holding, the alloy containing 5 wt.% Mg excess was also held at the foaming temperature for 180 s. The foam continued to expand, but the foam structure exhibited many large cells of irregular shape after. No drainage was seen in any of the foams containing 1, 2 and 5 wt.% Mg excess that was held for 140 s or 180 s.

Analysis of the 2D cell size distribution was done for the foams containing 1, 2 or 5 wt.% Mg excess that were held for 140 s, see Fig. 5 a-c. The foam with 1 wt.% Mg addition shows an uniform cell size distribution and a mean cell size D of 3.21 ±0.15 mm. In contrast, the analysis reveals a non-uniform cell size distribution for the foam with 2 and 5 wt.% Mg excess with slightly lower mean cell sizes. The foam containing 5 wt.% Mg excess was held for 180 s and exhibits even larger mean cell size D, see Fig. 5d. There is no trend in the cell size distribution as a function of Mg addition, but there is a significant increase in the cell size when the time of holding of the foams is increased to 180 s.

The 2D cell circularity analysis (Fig. 6a-c)of the foams with 1, 2 and 5 wt.% Mg excess held for 140 s shows that a large number of cells are not equiaxed and this number increases with an increase in Mg. The foam with 5 wt.% Mg excess and held for 180 s also contains non-equiaxed large cells. The cell circularity of the foam containing 0.13 wt.% Mg obtained after 100 s foaming (Fig.3d) is incomparable with that of the foams with 1, 2 and 5 wt.% Mg ex-

cess. The former showed mostly equiaxed cells throughout the foam cross section. Figure 7 shows the comparative plot of circularity of the foams containing 0.13 wt.% Mg and 1wt.%Mg. The mean circularity value of the former is 0.85±0.012 while the later is 0.69±0.004.

For comparison of cell structure, an X-ray tomographic reconstruction of a transverse section of the foam with 0.13 wt.% Mg obtained after 100 s of holding is compared to reconstructions of foams containing 1, 2 or 5 wt.% Mg excess and foamed for 140 s (Fig. 8). Clearly, the foams with higher Mg contents exhibit a less equiaxed cell structure and less uniform distribution in comparison to the foam with 0.13 wt.% Mg. All the elongated cells are associated with remnants of broken cell walls, which indicates that cell wall rupture has taken place and has caused cell coalescence. In addition, the periphery of the foams is denser for 2 and 5 wt.% Mg addition, which reflects the pronounced collapse of cells taking place on the foam surface during solidification.

The foams containing 1 wt.% Mg excess obtained by foaming for 100 s and 140 s were chosen for a compressibility and energy absorption study due to their stability and uniform cell structure even after longer holding. Foams with 2 and 5 wt.% Mg excess possess more broken cell walls and are therefore not taken for mechanical property evaluation. For the compression studies, the 5 Nos. of samples were sliced into cubes of (25×25) mm^2 size from the top to the bottom of both foams that we call as *foam-1* and *foam-2* obtained after 100s and 140s holding respectively. The densities of each sample obtained in this way vary from 0.19 to 0.37 $g{\cdot}cm^{-1}$ (table 1). Figure 9a presents a closer view of the cross sections of a re-melted Al scrap foam containing 1 wt.% Mg excess, foamed for 140s and having a density of 0.19 $g{\cdot}cm^{-1}$ (*foam-2*). It is apparent that the cell structure is reasonably uniform.

Figures 9b and c show the structures for Cymat and Alporas foams with densities of 0.38 $g{\cdot}cm^{-1}$ and 0.22 $g{\cdot}cm^{-1}$respectively[14]. Figure 9d presents the structure of a Formgrip

198 foam with a density of 0.30 $g \cdot cm^{-1}$[15]. Although the foam densities are not comparable in
199 this image, a fair comparison of the foam structures can be made. It is well known that Cymat
200 foams display a much wider distribution of cell sizes than Alporas foams. If foams with simi-
201 lar densities are compared (all at roughly 0.2 $g \cdot cm^{-1}$) then the Cymat foam is coarser with
202 cells of a mean diameter of roughly 7–8 mm [14], compared to 3–4 mm for Alporas[14, 16-
203 17]. The cell size and uniformity for the foam made from re-melted Al scrap are unlike those
204 for the Cymat foam (made by bubbling gas into an Al-Si melt using SiC particles to stabilise
205 the bubbles) and more closely resemble those for Alporas [18] and Formgrip foams
206 [15],which are also made by TiH_2 decomposition in a Al alloy melt.

207 Figure 10a shows a 3D tomography of the exemplary shape and dimension of one of the foam
208 samples (*foam 1*, density is 0.37, holding time is 100s) used for compression testing. The
209 compressive stress-strain curves for the re-melted Al scrap foams are given in Fig. 10b. As
210 expected, there is an increase in the yield stress with increasing foam density. Table 1 pre-
211 sents these values as measured from the initial maximum. Beyond yielding, the stress-strain
212 curves undulate (the load rises and then drops sharply). These events are coupled with obser-
213 vations during compressive testing of brittle fracture of the cell walls after collapse and sig-
214 nificant crumbling (images not shown).

215 Table 1 also presents data for the energy absorbed per unit volume (in $MJ \cdot m^{-3}$) at 50% strain.
216 The efficiency of energy absorption across the range of densities is roughly 80–85%. For this
217 level of compressive strain, which is below the onset of densification (at typically 65–70%
218 strain), the flat plateau for the Alporas foam means that the efficiency is >90%. For the Cy-
219 mat foam, it is <70% owing to the steadily increasing stress with strain, see Fig.10c [14, 19].

220

221 **4. Discussion**

222 The aforementioned results clearly show that the microstructure of re-melted Al scrap alloy is
223 modified by the addition of Mg. The long oxide filaments present in the alloy matrix are
224 fragmented into smaller films and get distributed in the matrix due to addition of Mg in ex-
225 cess to the level in the base alloy (Fig.1 a,b).Fragmentation occurs due to thinning of oxides
226 caused by their reaction with Mg, which also improves the wetting of oxides by liquid alu-
227 minium [20]. In this reaction, reaction products such $MgAl_2O_4$ and MgO particles format ox-
228 ide-matrix interfaces. However, adding higher amounts of Mg (>1 wt.%) causes formation of
229 Mg_2Si and does not increase the formation of $MgAl_2O_4$ particles in the matrix.

230 The amount of oxide present in the alloy is 0.11±0.01 wt.% based on the oxygen content in
231 the swarfs (machining chips and turnings). No heat treatment was carried out to increase the
232 oxygen content in the swarfs as it was done in previous studies [11-12]. If all the oxygen is
233 converted into oxides, then this corresponds to 0.23 wt.% Al_2O_3. After melting the swarfs, the
234 concentration of oxides in the alloy would certainly increase during prolonged holding of the
235 swarfs (loose chips and turnings) at high temperature. The oxide content measured in the re-
236 melted scrap alloy is < 1 wt.%. Magnesium added to the melt for conditioning reacts with
237 aluminium oxide and forms $MgAl_2O_4$ (spinel) and MgO as already small amounts of Mg
238 (0.02 wt.%) can destabilize Al_2O_3 to form $MgAl_2O_4$ spinel. At higher Mg concentrations
239 (0.06 wt.%),MgO is formed at temperatures around 1000 K (727 $^{\circ}$C)[20]. In our study, the
240 Mg concentrations 0.13% wt.% and those increased by 1, 2 and 5 wt.% led to the formation
241 of $MgAl_2O_4$ and MgO, but there is no significant increase in $MgAl_2O_4$ or MgO on increasing
242 the Mg concentration, which could be attributed to the large size of the oxide films. Vinod-
243 Kumar et al. have shown that complete reaction of Mg with the oxides to form large volumes
244 of $MgAl_2O_4$ requires a higher oxide concentration (e.g. 5 wt.% of SiO_2) and the oxides should
245 be finer in size (mean size is 44 μm in that case)[7]. In the present work, the reaction is in-
246 complete due to large sized oxides and therefore the excess Mg reacts with Si (10 wt.% con-

tent in the alloy) to form Mg_2Si during solidification. Therefore, adding more than 1 wt.% Mg during conditioning of the melt is not useful in fragmenting the oxide films or distributing them in the matrix to a greater extent.

The uniform and equiaxed cell structure and good expansion of re-melted Al scrap alloy foam without the addition of excess Mg (Fig. 3a, content only 0.13 wt.% Mg) indicates than long oxide filaments can act as a stabilizing agent but only for a shorter period (~100 s). Holding the liquid foam for 140 s caused collapse in the cells due to drainage, see Fig. 3b. Fragmentation of long oxide filaments into short films and their distribution in the matrix has significant impact on the foaming behaviour particularly on expansion and stability upon longer holding. The equally distributed cell structure as we could see in the foam containing 1 wt.% Mg (Fig. 4a) may be attributed to the fragmentation of long oxide filaments into shorter oxide films and good wetting aided by $MgAl_2O_4$ particles.

Shape irregularities, i.e. non-equiaxed cells, are found frequently for foams containing 2 or 5 wt.% Mg excess. Even foams with 1 wt.% Mg show more non-equiaxed cells (based on the mean circularity values shown in Fig.7) in comparison to the foam with 0.13 wt.% Mg, but not as significantly as for 2 and 5 wt.%. Assumptions were made that the increase in the viscosity of melt (containing free Mg) during stirring and admixing the blowing agent [21] could be a reason for the formation of a non-equiaxed cell structure. Incidentally, Alporas foams that are made from a highly viscous melt produced by admixing Ca and stirring for as long as 15 to 20 min [18]exhibit an equiaxed cell structure. Therefore, the non-equiaxed cell structure here should be rather attributed to the rupture of cell walls during solidification. Even during solidification the phenomenon of solidification expansion (SE) [22] can occur, which leads to cell wall thinning due to stretching and consecutive rupture and coalescence. This is clearly evident from the remnants of broken cell wall observed in the 2D radioscopic images of foams (Fig. 7a-d). Mukherjee et al. have pointed out that partially broken cell walls are a

clear indication that rupture took place during solidification[22]. If rupture occurred in the liquid state the liquid metal in a broken film would be redistributed into the surrounding structure and the geometry would be re-adjusted to an equiaxed bubble without leaving any traces of the ruptured cell wall. During solidification, the increase in viscosity (caused by the increasing solid fraction) will not allow the melt to redistribute in the cell wall and attain equilibrium structure. The base alloy composition of the re-melted scrap investigated here is Al–10 wt.% Si and has a larger solid-liquid co-existence region than in the base material of Alporas foams that is almost pure Al.

However, non-equiaxed cells are seen more frequently in foams with higher Mg addition (1, 2 and 5 wt.%) than in the foam based on an alloy with just 0.13 wt.% Mg where cells are equiaxed and fewer broken cell walls are observed. This indicates that the viscosity increase during solidification is not only because of the increasing solid fraction but also due to the formation of Mg_2Si particles. Mg_2Si forms at higher concentration of Mg and its volume fraction increases with Mg concentration in the alloy (Fig. 2). Mg_2Si particles are large and blocky in shape as seen in the interior of a foam cell wall (Fig. 11).

The compressive stress-strains plot of re-melted aluminium alloy scrap foams of various densities containing 1 wt.% Mg excess show good strength but wavy strain plateaus, which point at brittleness of the foams. This brittle behaviour is to be expected as the base alloy (LM26) has very limited ductility (<1%) and this will decrease further with the presence of significant levels of oxide films resulting from re-melting the scrap chips.

Comparisons can be made with the stress-strain behaviour of commercial foams [17] which have been normalized with respect to the initial maximum stress (Fig. 10c). At first inspection, the undulating curves resemble that for Cymat foam in which the cell material is also brittle in nature (due to using a brittle Al-Si-SiC matrix alloy). However, unlike the Cymat foam, the stress does not continually rise with progressive strain and in this respect there is

297 similarity to the Alporas foam. The much flatter stress-strain curve for the Alporas foam is
298 attributed to the much more uniform density and pore structure [17],which facilitates for-
299 mation of multiple deformation bands that are uniformly distributed throughout the sample
300 and enables progressive collapse to occur both by the expansion of existing bands and the
301 formation of new ones. In contrast, deformation of the more irregular Cymat foam is highly
302 localized in bands (generally containing large pores or areas of low density), which then pro-
303 gress to other regions in the foam only after the cells in the band have reached the point of
304 densification.

305 The initial maximum yield strengths for Alporas foams with densities in the range of 0.2–
306 0.4 $g \cdot cm^{-1}$ typically vary between 1.4–2.4 MPa [14,16,19]. For Cymat foams, the comparable
307 property is sensitive to the foaming direction and the gravity vector. For a comparable direc-
308 tion to that tested in this work, strengths between 1.2–5.0 MPa were observed [16]. The
309 strengths for the scrap and Cymat foams are of course higher than that for the Alporas foam
310 due to the higher inherent strength of the matrix material which is estimated to be 120–
311 170 MPa for Alporas, 310–390 MPa for Cymat [14,17] and 290–310 MPa for the foamable
312 re-melted scrap alloy(calculated as part of this study from hardness measurements of the
313 foamable base material containing 1 wt.% Mg).

314 Predictions for the yield strength using either the approach of Ref.[14] or [16] and typical
315 matrix strength data as given above reveal higher “knockdown” factors (i.e. deviations from
316 the predicted properties) for the Cymat foam than for either the Alporas or scrap-based
317 equivalents. This supports prior hypotheses that relate these larger reductions in the expected
318 strength (and indeed the stiffness) observed in the Cymat foam to the greater anisotropy, het-
319 erogeneity and variations in density as well as a higher occurrence and severity of cell wall
320 defects (wiggles, holes, fractures), which result from both the foaming and foam handling
321 processes specific to Cymat foam [14,16].

5. Conclusions

- Mg additions in excess to the level contained in the base scrap alloy (0.13 wt.%) promote fragmentation and good distribution of oxides in the aluminium matrix. Formation of $MgAl_2O_4$ (spinel) of octahedral morphology on the surface of the oxides can be observed. Increasing Mg additions to 2 or 5 wt.% do not cause any notable further increase in the formation of $MgAl_2O_4$ or MgO compared to 1 wt.% addition and no further fragmentation of oxides or better distribution could be seen. However, an increase of Mg addition causes the formation ofMg_2Si during solidification.
- Foaming re-melted Al scrap alloy without any additional Mg in excess to the 0.13 wt.% in the base alloy led to an equiaxed cell structure, indicating that long oxide filaments can act as stabilizing agent, but only if holding time was limited to 100 s. Upon longer holding (e.g. 140 s), strong drainage in the foam set in and foam collapse was observed.
- With 1 wt.% Mg excess, the expansion and the stability of foam upon longer holding (140 s) is good due to fragmentation and good distribution of oxides. The foam with 1 wt.% Mg excess showed very good cell structure and a uniform cell size distribution.
- Increasing Mg additions to 2 or 5 wt.% led to stability even after longer holding but the expansion slowed down. Corresponding foams showed a less equiaxed cell structure caused by cell wall rupture and coalescence occurred during solidification than foams without or with just 1wt.% Mg addition.
- Solidification expansion and the increase in viscosity during solidification of a foam are the reason for non-equiaxed cell structures. In foams that contain 2 or 5 wt.% Mg excess, the increase in viscosity during solidification and the formation of non-equiaxed cells are still more pronounced due the formation of Mg_2Si during solidification.

- During compression tests, foams with 1 wt.% Mg excess (having optimum cell structure) of various densities exhibit brittle crumbling of the cell walls, which is typical compressive behaviour for a low-ductility Al-Si casting alloy containing significant levels of oxides. However, their uniform pore structure leads them to have flatter compression stress plateaus, higher energy absorption efficiencies and a reduced "knockdown" in properties, which is comparable with that of Alporas foams made in the same way. Therefore, foams made from re-melted alloy scrap could offer the same performance as Alporas foams but at a lower cost.

References

1. J. Banhart, Prog. Mater. Sci., 2001. vol. 46, pp. 559-632.
2. L. Drenchev, J. Sobczak, S. Malinov, W. Sha, Mater. Sci. Technol., 2006, vol. 22, pp. 1135-47.
3. S. W. Ip, S.Y.Wang, J. M. Toguri, Can. Metall. Q, 1999, vol. 38, pp. 81-92.
4. J. Banhart, J.Met., 2000, vol.52, pp. 22-27.
5. N. Babcsán, D. Leitlmeier, H.P. Degischer, Materialwiss. Werkstofftech., 2003, vol.34, pp. 22-29.
6. N. Babcsán, F.Garcia-Moreno, J. Banhart, Colloids Surf., A, 2007, vol.309, pp. 254-63.
7. G. S. Vinod kumar, M. Chakraborty, F. Garcia-Moreno, J. Banhart, Metall. Mater. Trans. A, 2011, vol.42, pp. 2898-908.
8. J. Banhart, Adv. Eng. Mater., 2006, vol.8, pp.781-94.
9. W. Ha, S. K. Kim, H.H Jo, Y.J Kim, Mater. Sci. Technol., 2005, vol.21, pp. 495-99.
10. M. Haesche, D. Lehmhus, J. Weise, M. Wichmann, I. C. M. Mocellin, J. Mater. Sci. Technol., 2010, vol.26, pp. 845-50.

11. G. S. Vinod Kumar, K. Heim, F. Garcia-Moreno, J. Banhart, A. R. Kennedy, Adv. Eng. Mater., 2013, vol.15, pp.129-33.
12. G. S. Vinod Kumar, K. Heim, F. Garcia-Moreno, J. Banhart, A. R. Kennedy,. Int. J. Mater. Res., 2015, vol.106, pp. 978-87.
13. M. Mukherjee, U. Ramamurty, F. Garcia-Moreno, J. Banhart, Acta Mater., 2010, vol.58, pp. 5031-42.
14. E. Andrews, W. Sanders, L.J. Gibson, Mater. Sci. Eng. A, 1999, vol.270, pp. 113-24.
15. V. Gergely and B. Clyne, Adv. Eng. Mater., 2000, vol.2, pp. 175-78.
16. O.Olurin, N. Fleck, M. Ashby, Mater. Sci. Eng. A, 2000, vol.291, pp. 136-46.
17. A. E. Simone and L.J. Gibson, Acta Mater., 1998. vol.46, pp. 3109-23.
18. T. Miyoshi, M. Itoh, S. Akiyama, A. Kitahara, Adv. Eng. Mater., 2000, vol.2, pp. 179-83.
19. U. Ramamurty, and A. Paul, Acta Mater., 2004, vol.52, pp. 869-76.
20. B.C. Pai, G. Ramani, R. M. Pillai, K. G. Satyanarayana, J. Mater. Sci., 1995, vol.30, pp. 1903-11.
21. S.Y. Kim, Y.S. Um, B.Y. Hur, Mater. Sci. Forum, 2006, vol. 510-511, pp. 902-5, 2006
22. M. Mukherjee, F.Garcia-Moreno, J. Banhart, Scripta Mater., 2010, vol.63, pp. 235-38.

Table Caption

396 Table 1. Mechanical properties for scrap foams

397

398 Figure Captions

399 **Fig.1** SEM micrographs of re-melted aluminium scrap alloy. (a) As received (0.13 wt.%
400 Mg), (b) with 1 wt.% Mg excess, (c) $MgAl_2O_4$ particles on the surface of an Al oxide
401 film, (d) octahedral morphology of $MgAl_2O_4$ spinel particles, (e) energy dispersive
402 spectrum of aluminium oxide, $MgAl_2O_4$, Fe-based and Cu-based intermetallics present
403 in the alloy.

404 **Fig.2** XRD plots of re-melted aluminium scrap alloy with various Mg concentration.

405 **Fig.3** X-ray tomographic reconstructions of longitudinal cross sections of foams made from
406 scrap alloy containing 0.13 wt.% Mg and produced by uninterrupted foaming in an
407 alumina crucible at 973 K (700 °C) for (a) 100 s (b) 140 s. (c) 2D cell size distribu-
408 tion and (d) Circularity vs. equivalent diameter of the cells for the foam held for
409 100 s.

410 **Fig.4** X-ray tomographic reconstructions of longitudinal cross sections of scrap alloy foams
411 produced by uninterrupted foaming in an alumina crucible at 973 K (700 °C) for 140 s.
412 (a) 1 wt.% Mg, (b) 2 wt.% Mg, (c) 5 wt.% Mg and (d) foam containing 5 wt.% Mg
413 held for 180 s.

414 **Fig.5** 2D cell size distributions for scrap alloy foams produced by uninterrupted foaming in
415 an alumina crucible at 973 K (700 °C) for 140 s. (a) 1 wt.% Mg addition, (b) 2 wt.%
416 Mg addition, (c) 5 wt.% Mg addition, (d) 5 wt.% Mg addition but 180 s holding time.

417 **Fig.6** Circularity vs. equivalent diameter of the cells in re-melted scrap alloy foams produced
418 by uninterrupted foaming in an alumina crucible at 973 K (700 °C) for 140 s. (a) to (d)
419 corresponding to Fig. 5.

420 **Fig.7** Comparison of circularity of foams containing 0.13 wt.% Mg (Fig.3d) and 1wt.%Mg
421 (Fig.6a). The mean circularity value (Gaussian fit) of the foam containing 0.13wt%Mg
422 is 0.85±0.012 and for the foam containing 1 wt.% Mg is 0.69±0.004.

423 **Fig.8** X-ray tomographic reconstructions of transverse sections of re-melted Al scrap alloy
424 foams produced by uninterrupted foaming in an alumina crucible at 973 K (700 °C). (a)
425 0.13 wt.% Mg held for 100 s, (b) 1 wt.% Mg addition, (c) 2 wt.% Mg addition, (d) 5

wt.% Mg addition, (b-d) held for 140 s. Arrows marks indicate the remnants of broken cell walls.

Fig.9 Foam macrostructures for (a) foam made from re-melted scrap, *foam 2* (1 wt.% Mg addition, holding time is 140s and density is 0.19 $g \cdot cm^{-1}$), (b) Cymat foam [3] (density = 0.38 $g \cdot cm^{-1}$), (c) Alporas foam [3] (density = 0.22 $g \cdot cm^{-1}$) and, (d) Formgrip foam (density = 0.3 $g \cdot cm^{-1}$) [4].

Fig.10 (a) 3D rendering of tomography of one of the test samples (*foam 1*, density is 0.37g/cc, holding time is 100s). (b,c) Compressive stress–strain plots for foams made from (b) Compressive Stress vs Strain plot of re-melted scrap foams containing 1wt.% Mg excess obtained after 100s and 140s holding (c) Compressive Stress vs Strain plot of Cymat (Alcan) foam and Alporas foam (taken from [17]).

Fig.11 SEM micrograph of re-melted Al scrap foam containing 2wt.% Mg excess showing Mg_2Si phases in the interior of a cell wall and oxide films at the gas solid interface.

Table 1. Mechanical properties for scrap foams

Foams	**Mg added excess to 0.13wt.% (wt.%)**	**Holding time (s)**	**density ($g \cdot cm^{-1}$)**	**yield strength (MPa)**	**$E_{abs}(MJ \cdot m^{-3})$**
foam 1	1	100s	0.34	5.63	2.36
			0.37	6.49	2.64
foam 2	1	140s	0.19	1.16	0.64
			0.24	2.10	1.07
			0.28	3.58	1.47

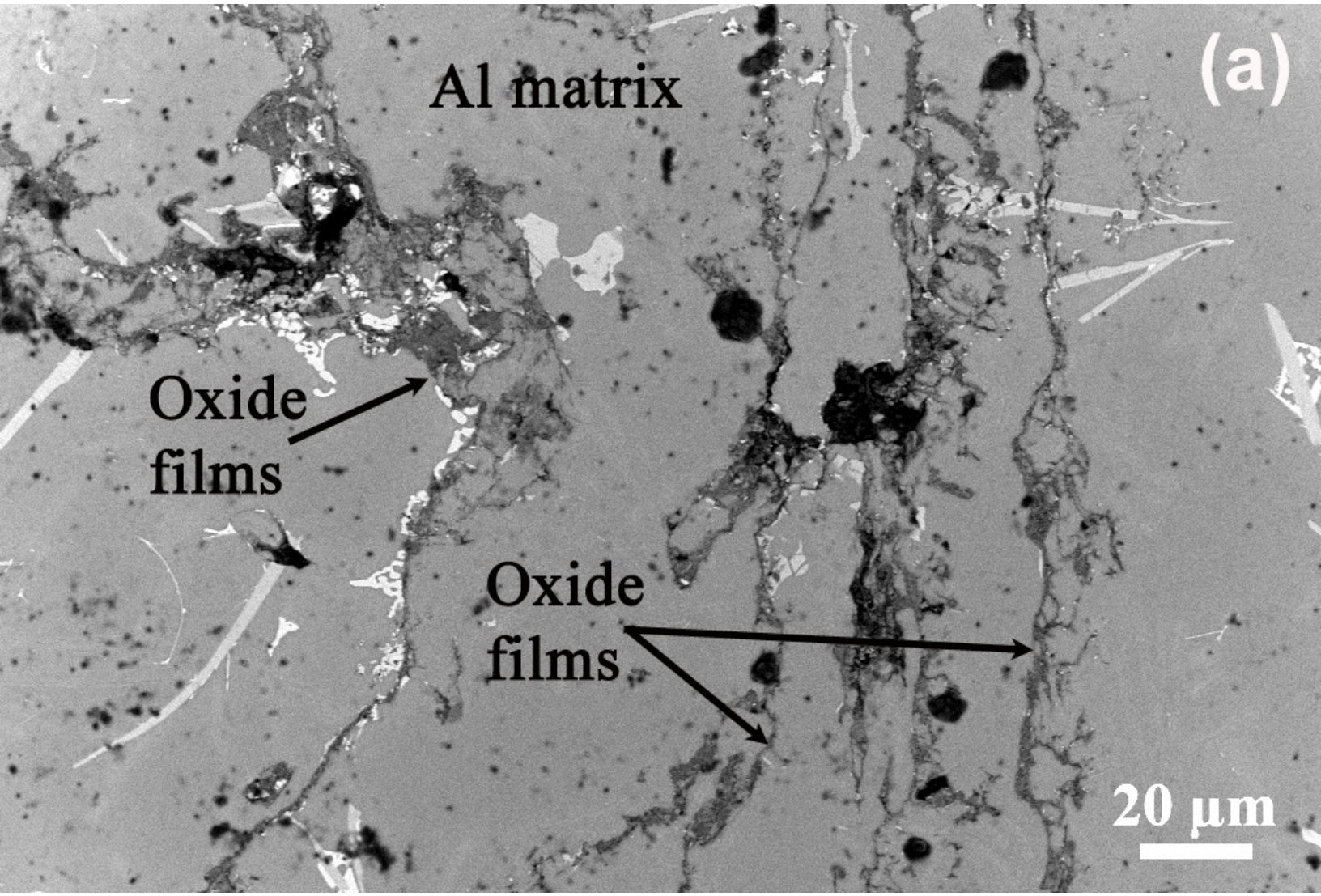
Al matrix
(a)
Oxide
films
Oxide
films
20 µm

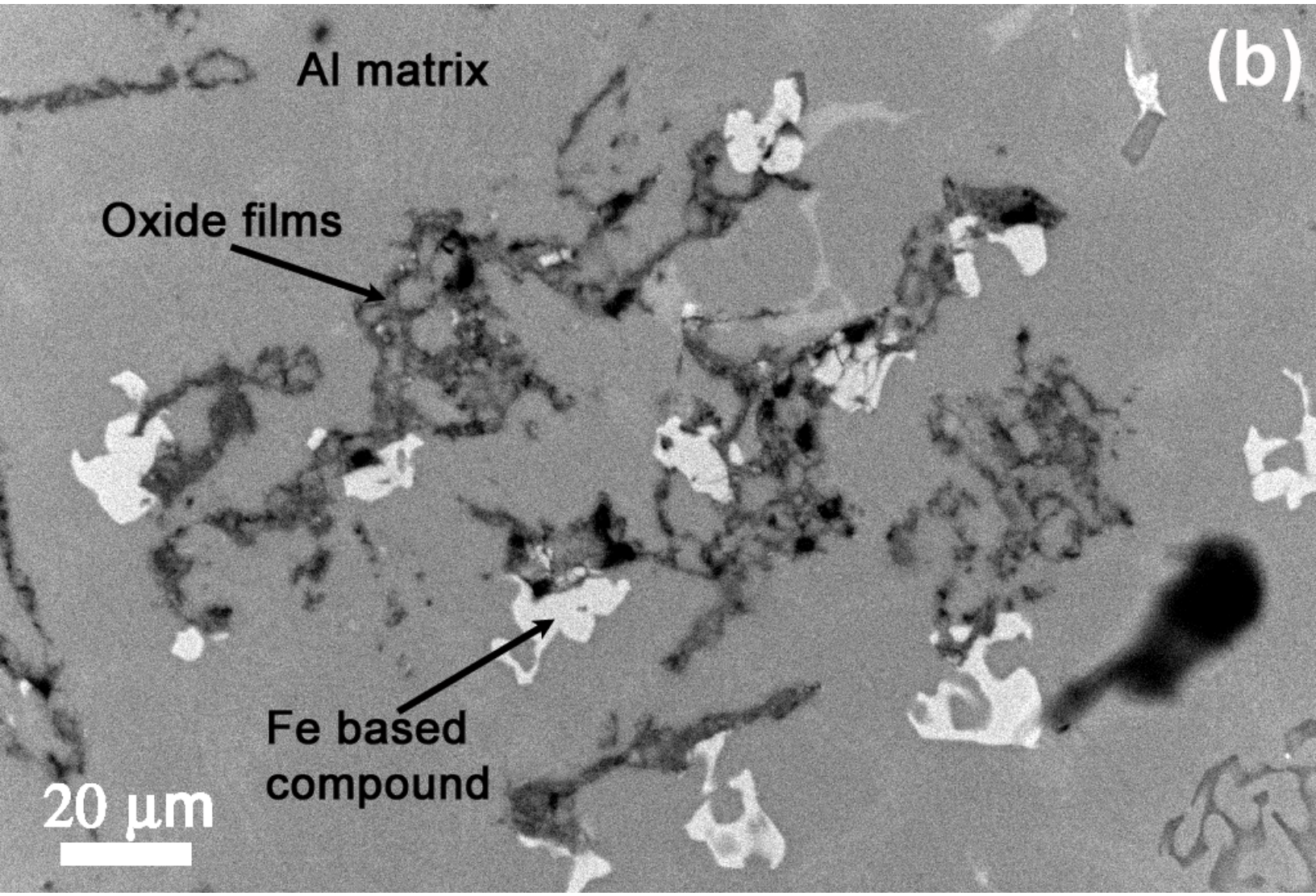
Al matrix
(b)
Oxide films
Fe based
compound
20 μm

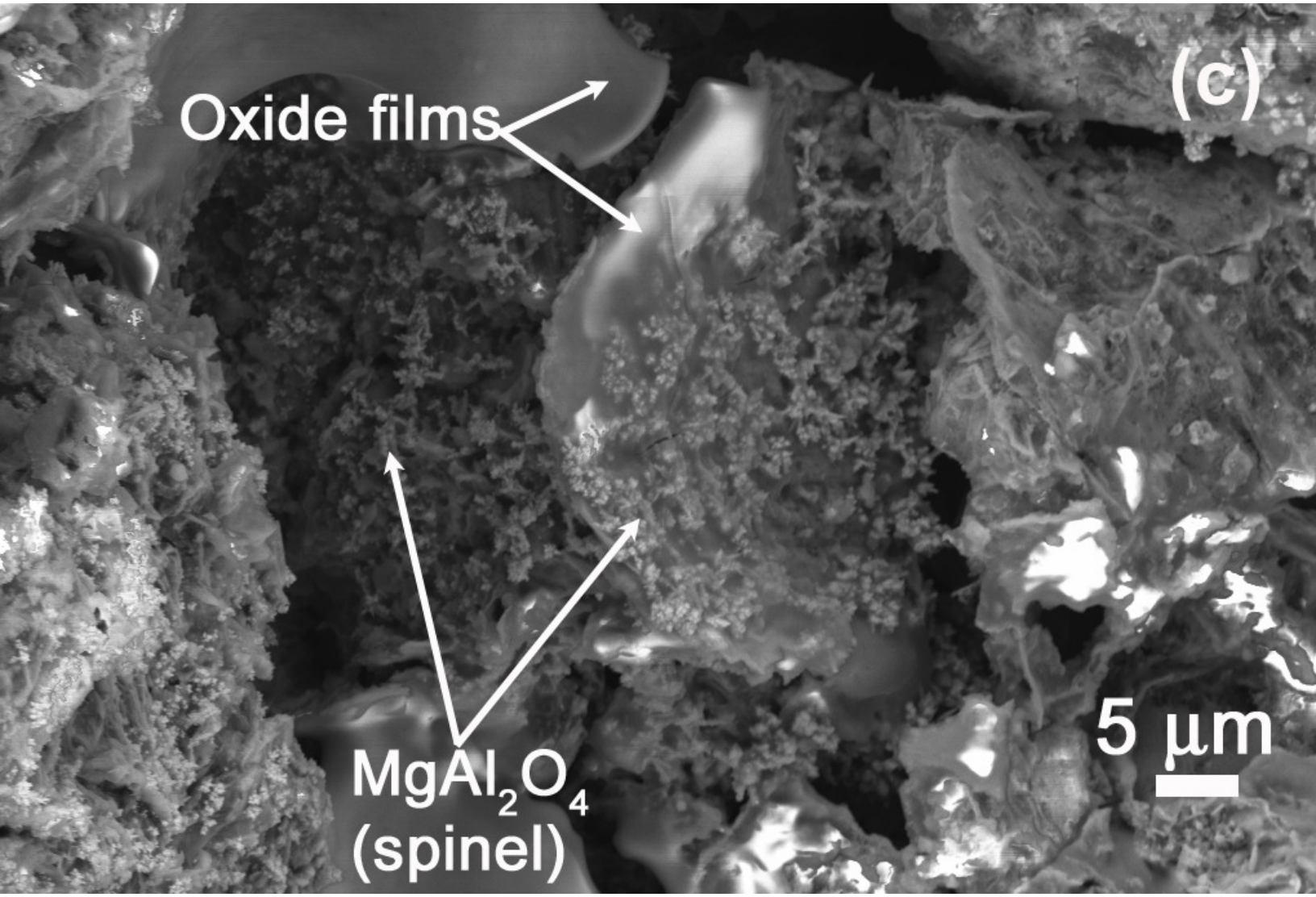
(c)
Oxide films
$MgAl_2O_4$
(spinel)
5 µm

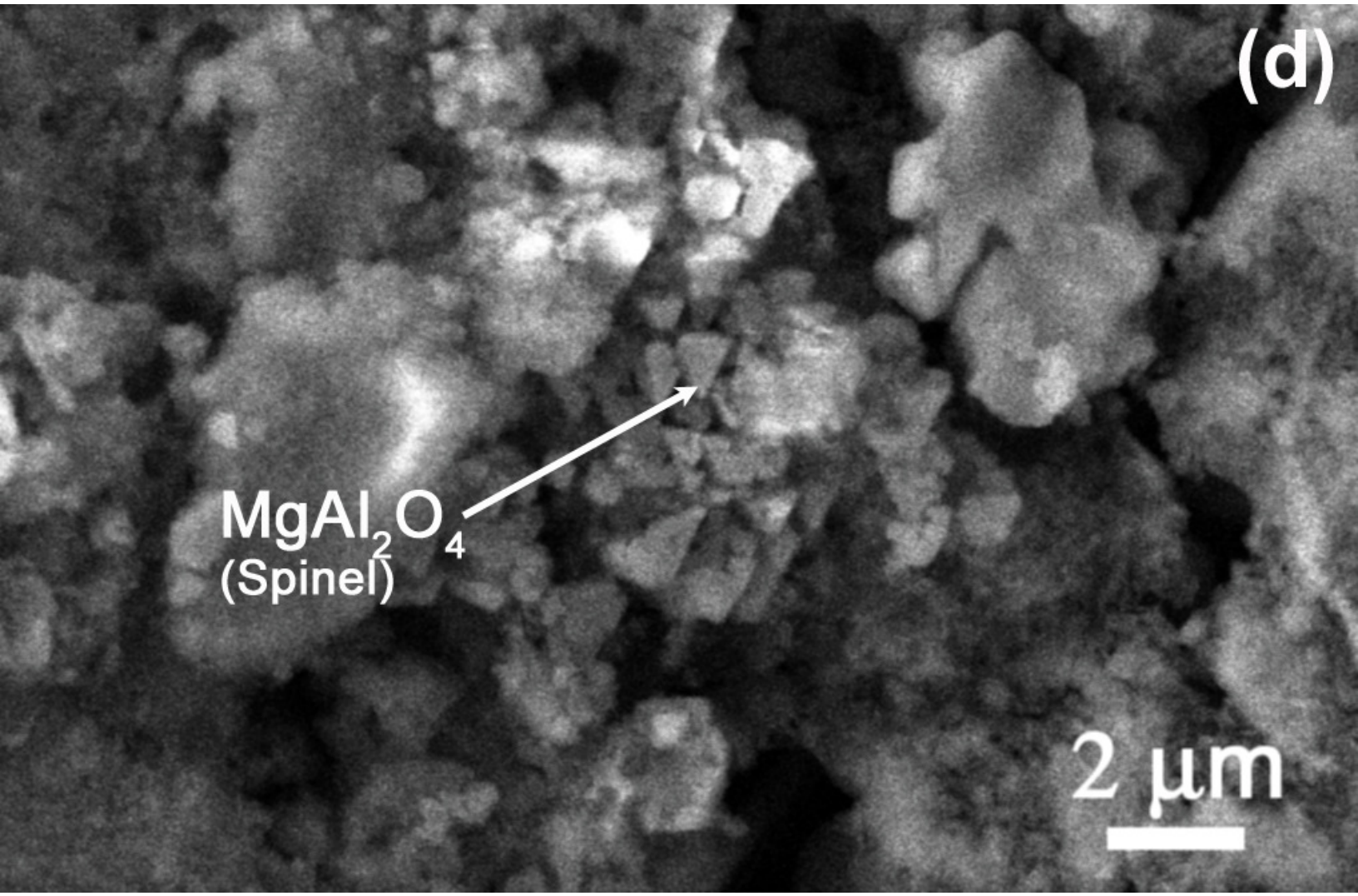
(d)
MgAl2O4
(Spinel)
2 µm

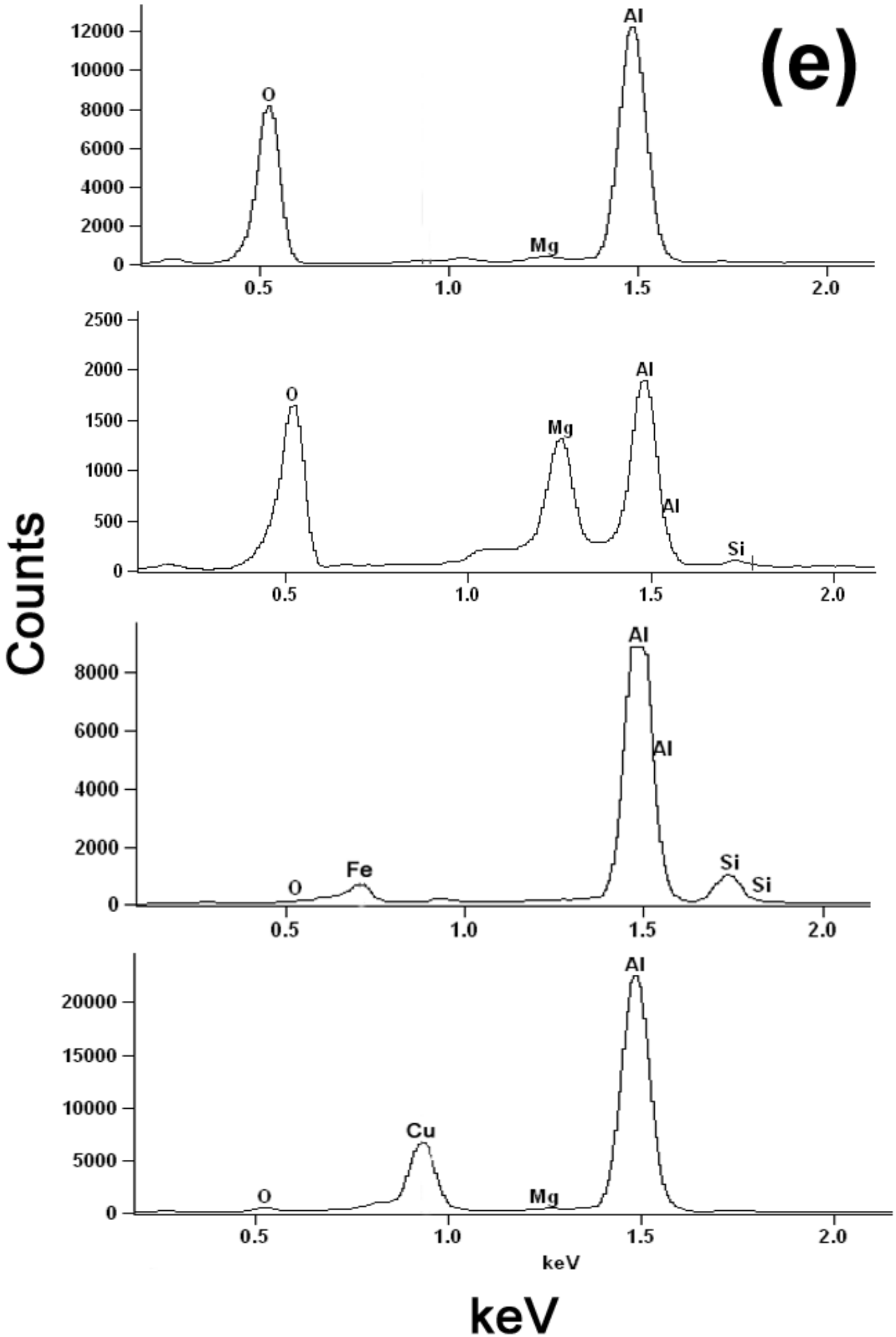
(e)
Counts
keV
O
Mg
Al
Si
Fe
Cu

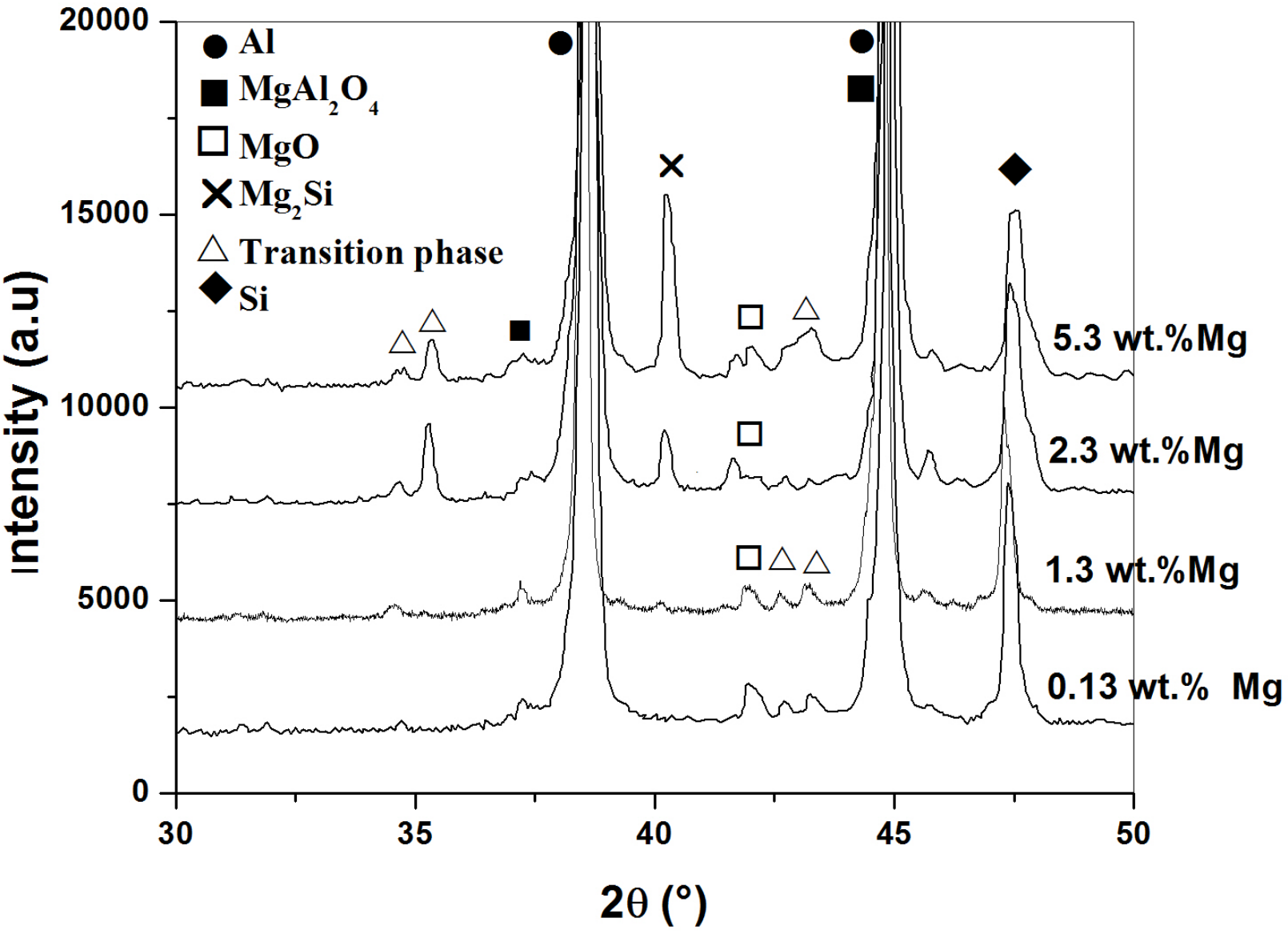
Al
MgAl2O4
MgO
Mg2Si
Transition phase
Si
5.3 wt.%Mg
2.3 wt.%Mg
1.3 wt.%Mg
0.13 wt.% Mg
Intensity (a.u)
2θ (°)
0
5000
10000
15000
20000
30
35
40
45
50

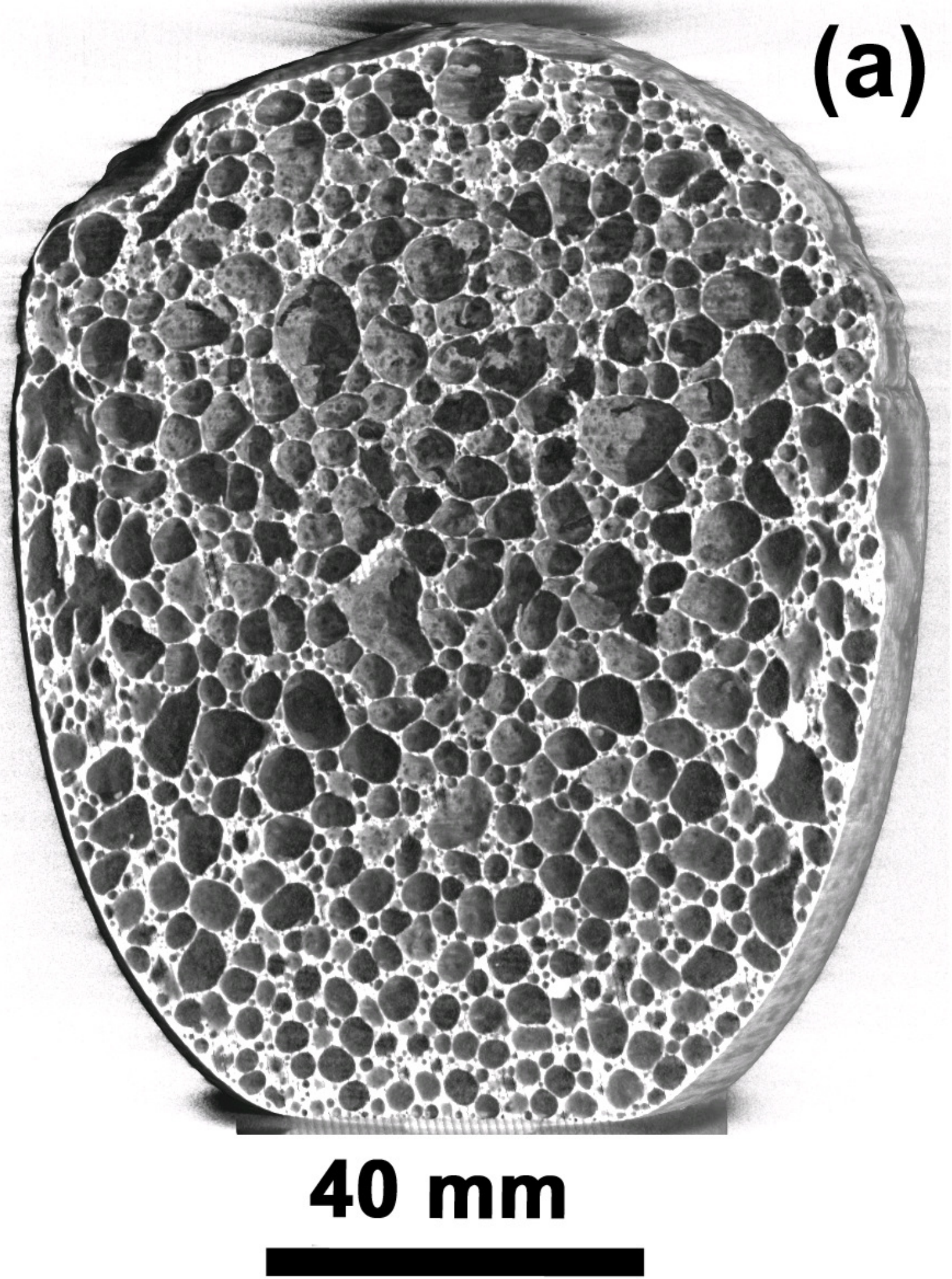
(a)
40 mm

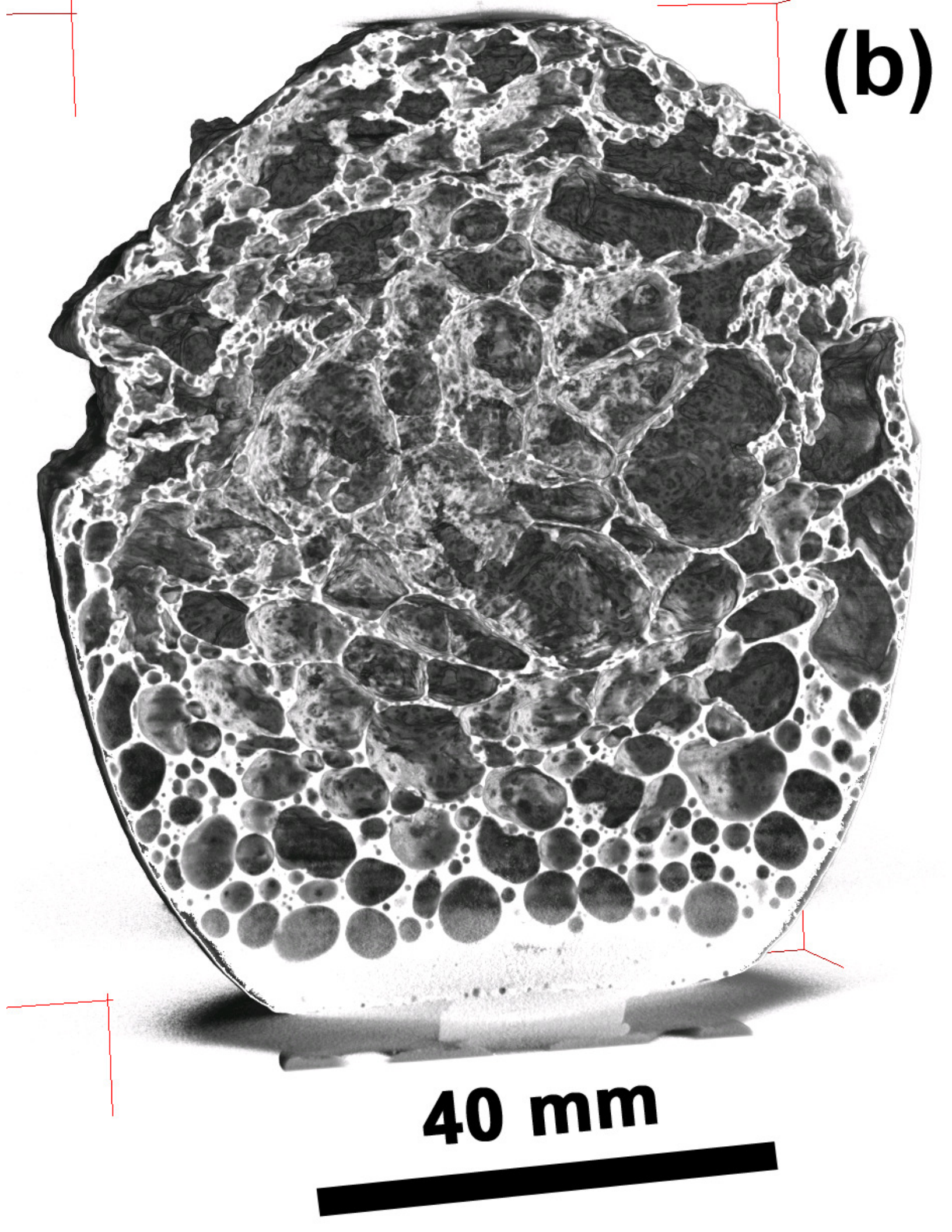
(b)
40 mm

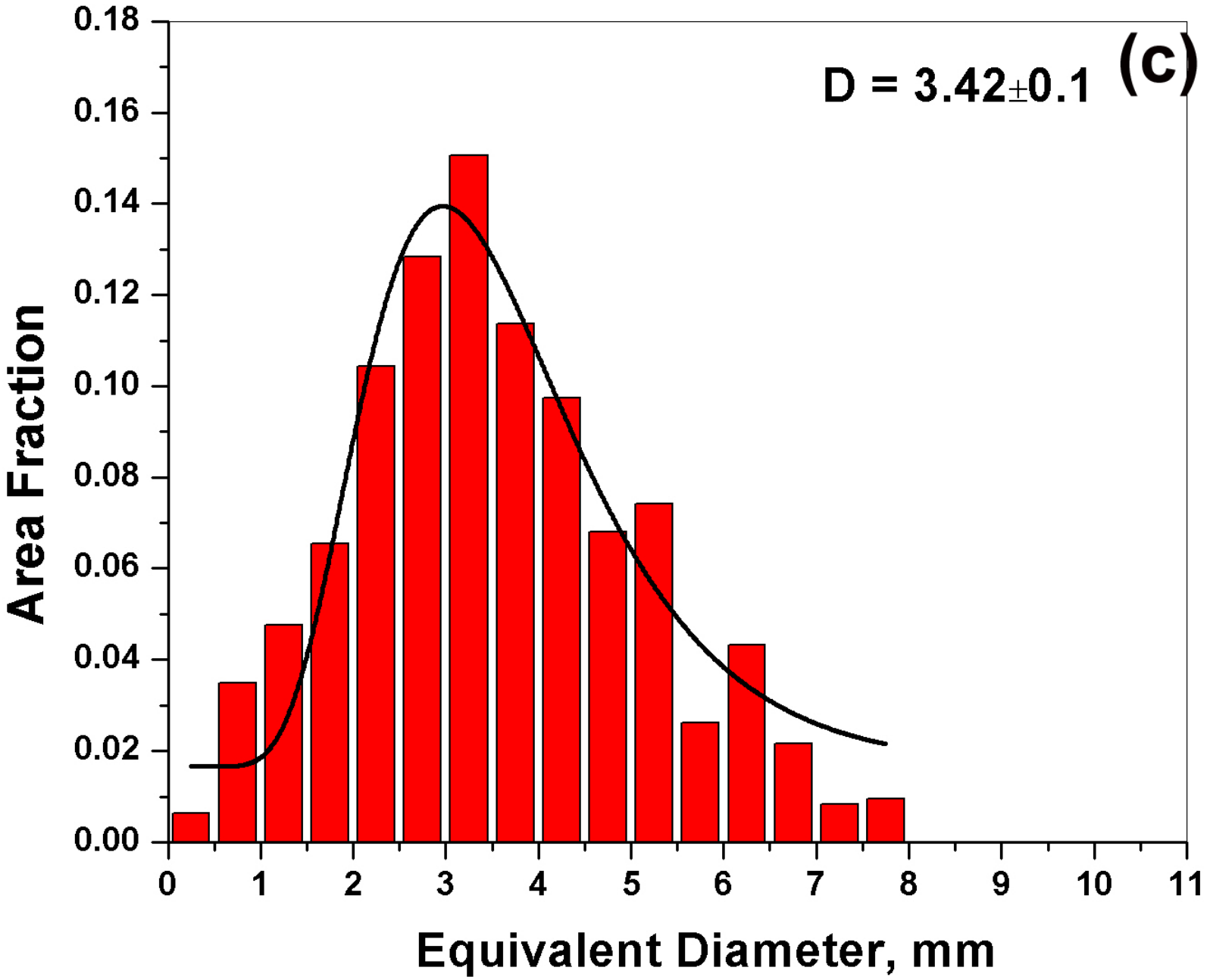
(c)
D = 3.42±0.1
Area Fraction
Equivalent Diameter, mm
0.00
0.02
0.04
0.06
0.08
0.10
0.12
0.14
0.16
0.18
0
1
2
3
4
5
6
7
8
9
10
11

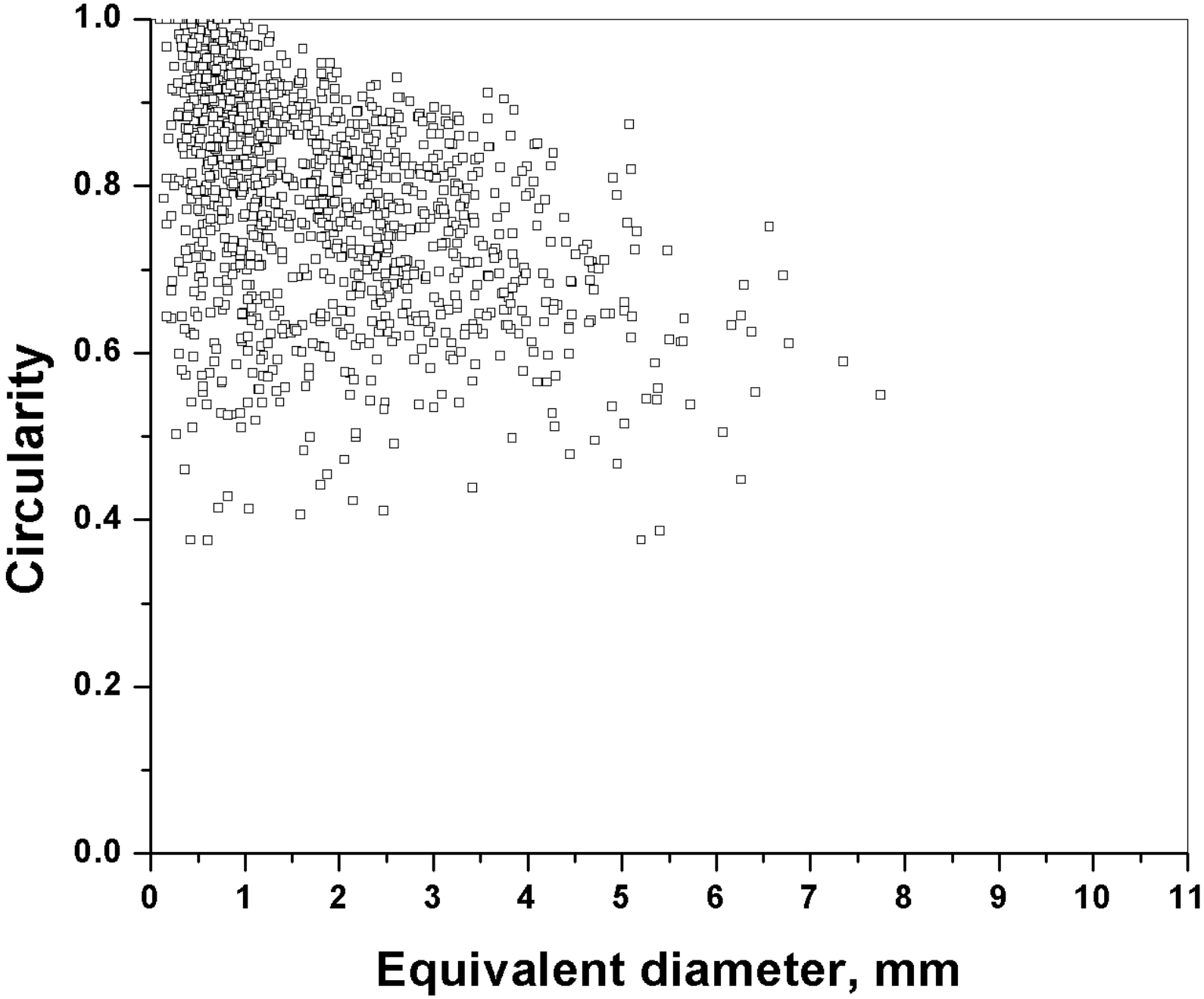
Circularity
1.0
0.8
0.6
0.4
0.2
0.0
0
1
2
3
4
5
6
7
8
9
10
11
Equivalent diameter, mm

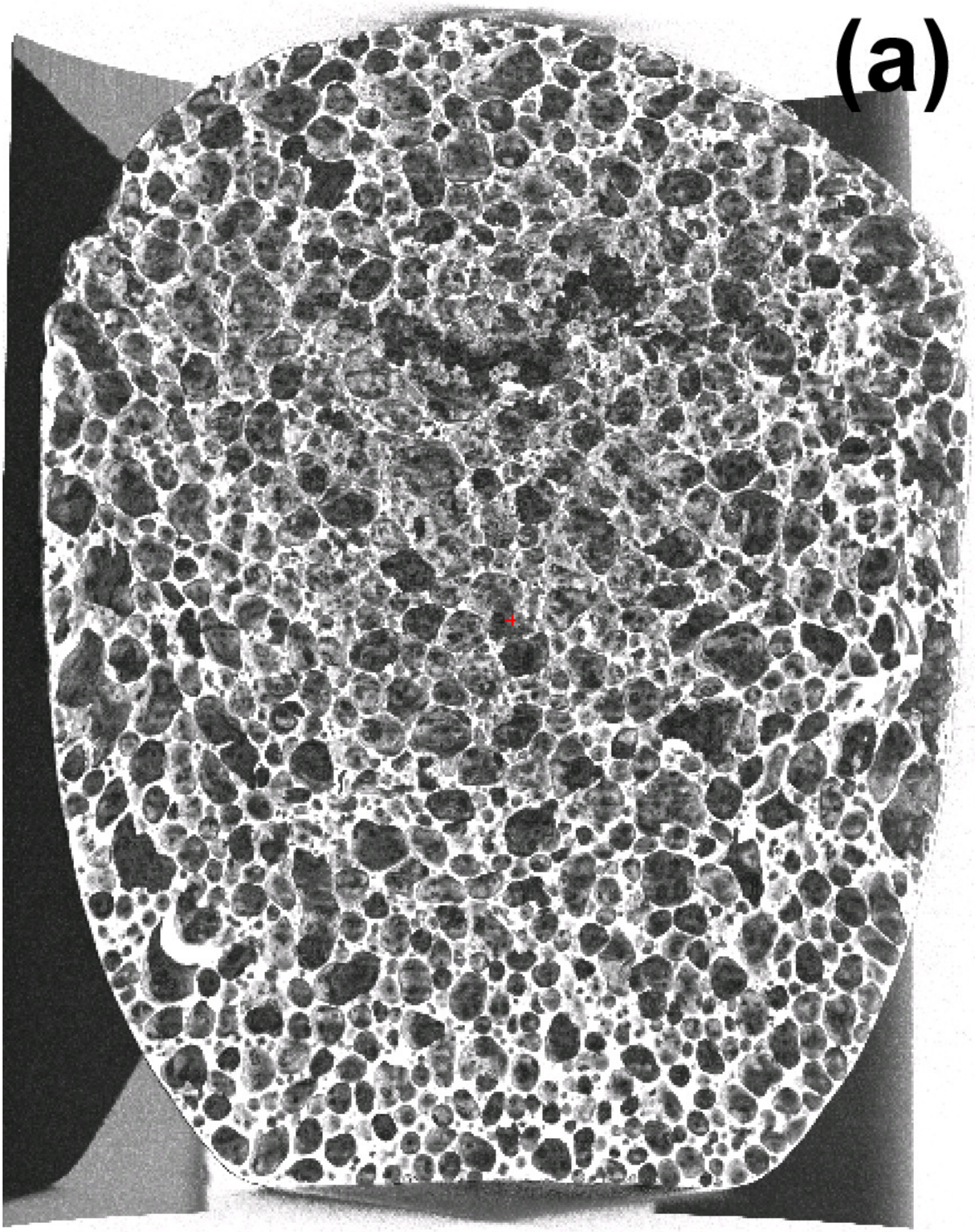
(a)
40 mm

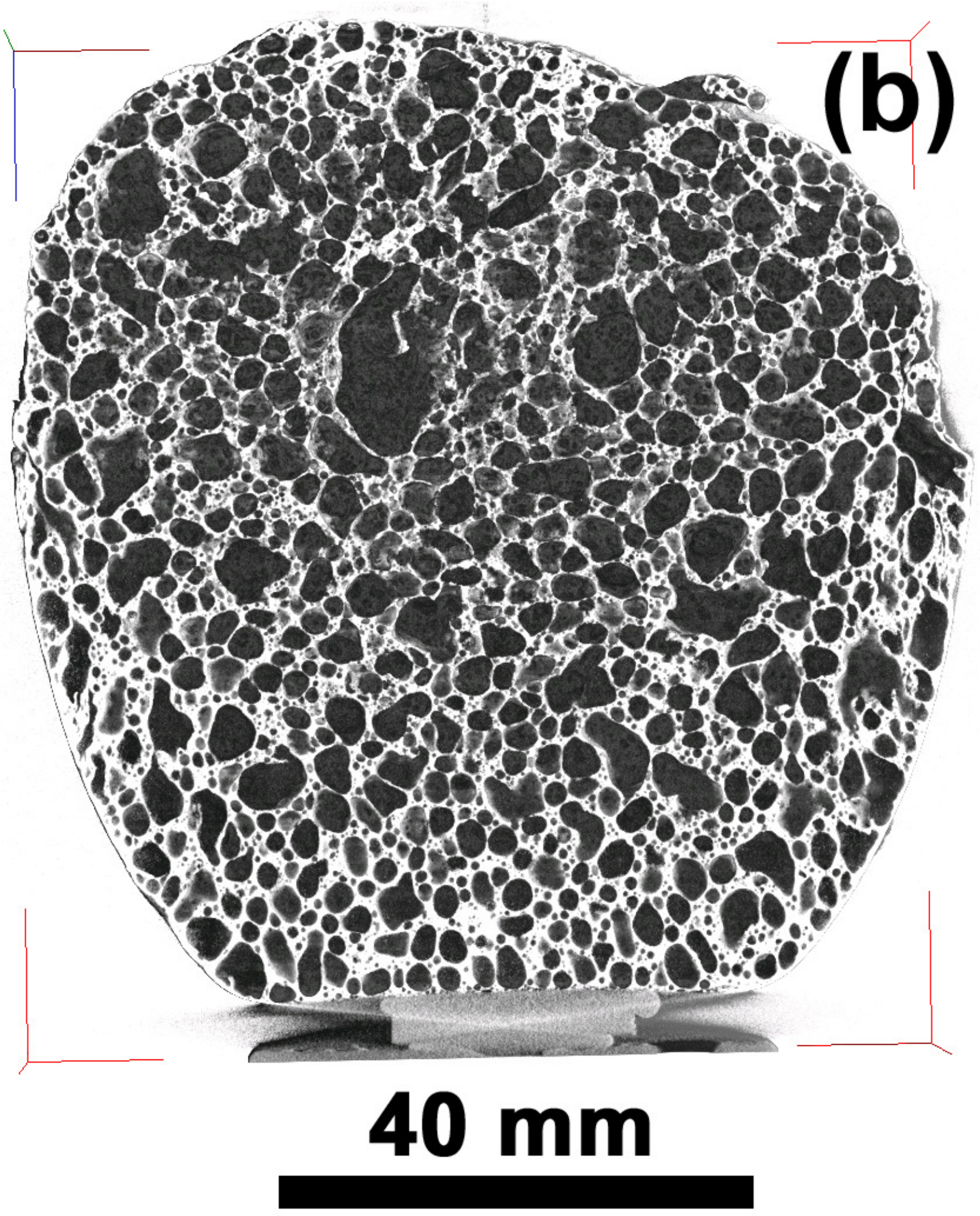
(b)
40 mm

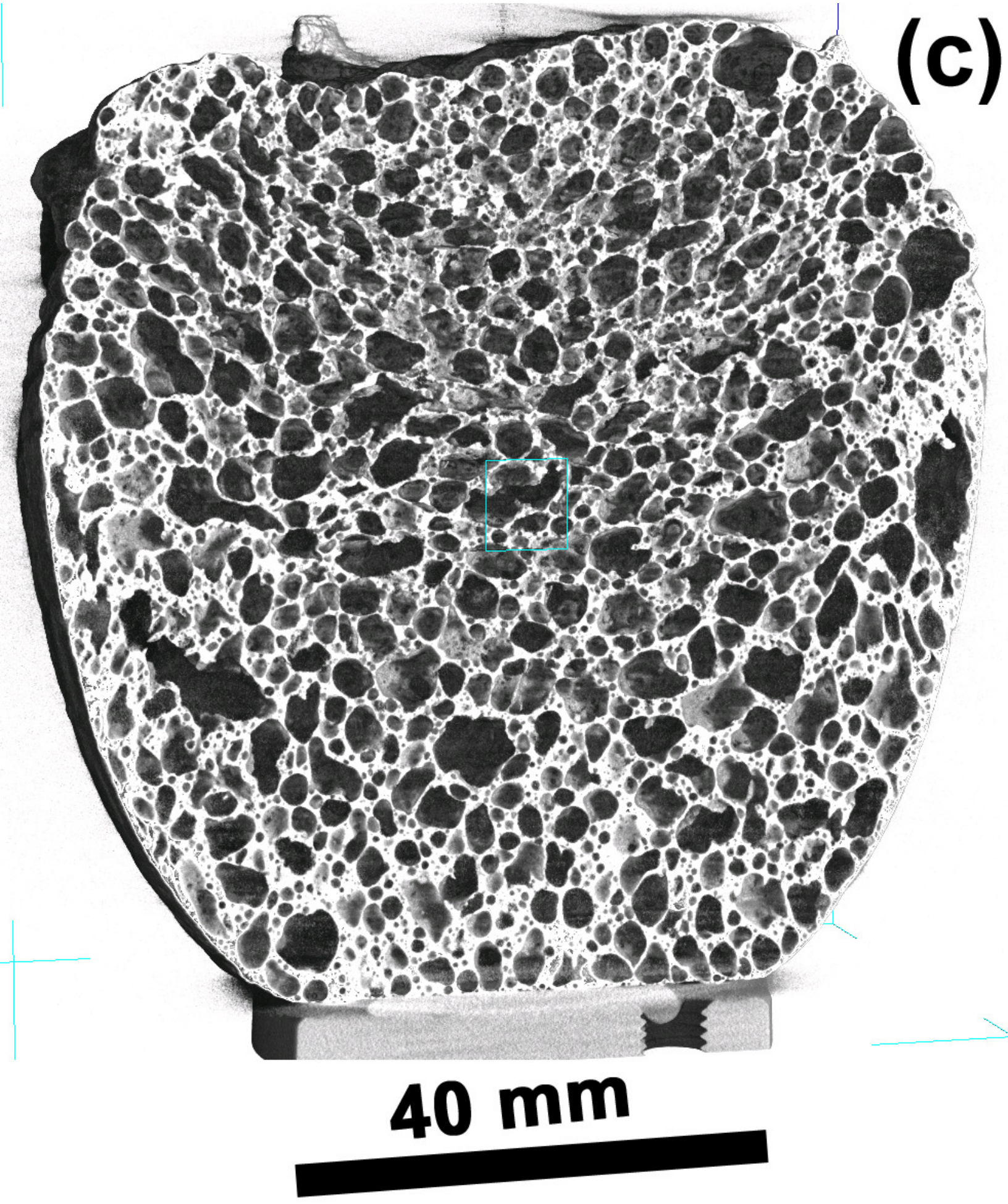
(c)
40 mm

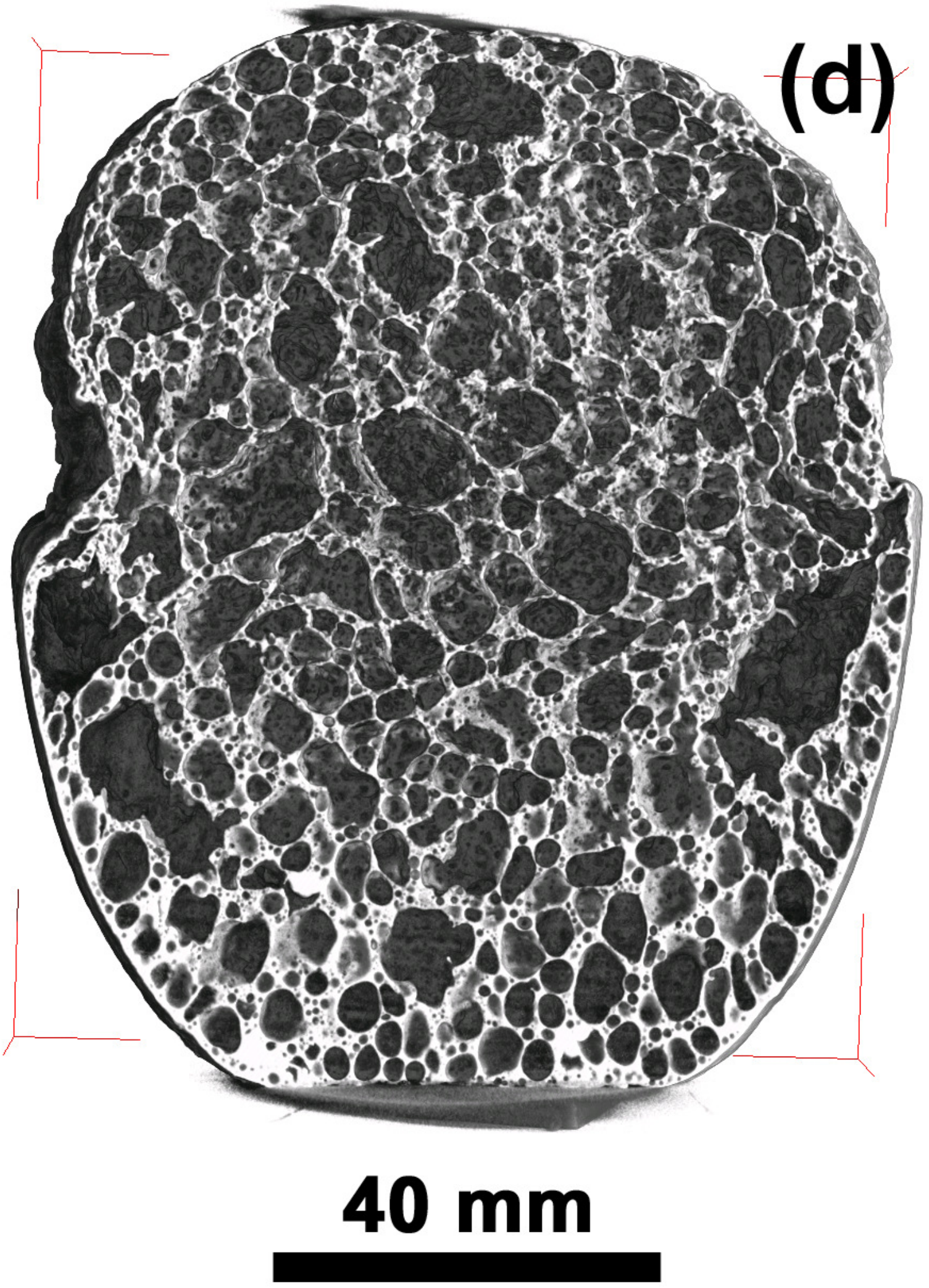
(d)
40 mm

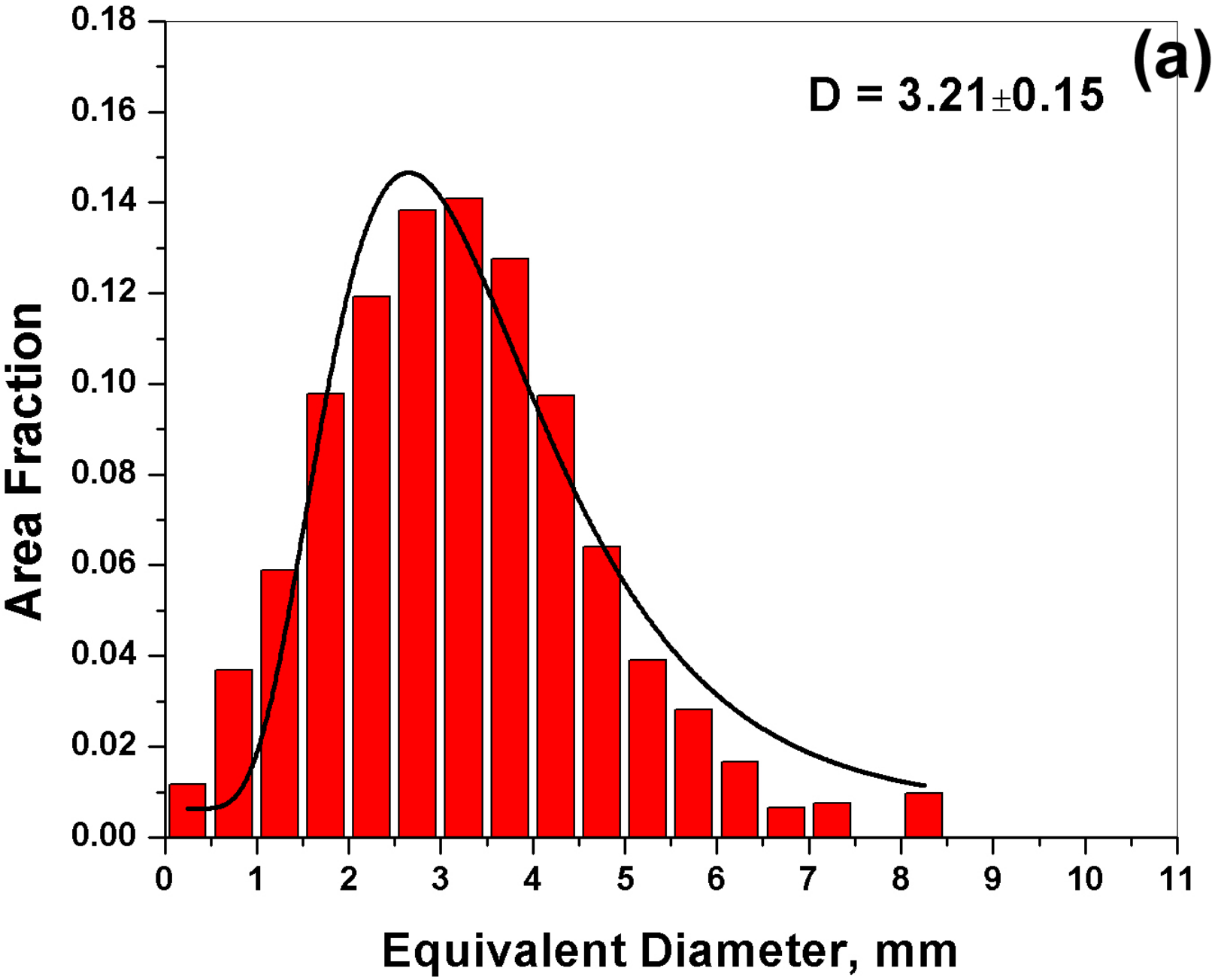
(a)
D = 3.21±0.15
Area Fraction
Equivalent Diameter, mm
0.00
0.02
0.04
0.06
0.08
0.10
0.12
0.14
0.16
0.18
0
1
2
3
4
5
6
7
8
9
10
11

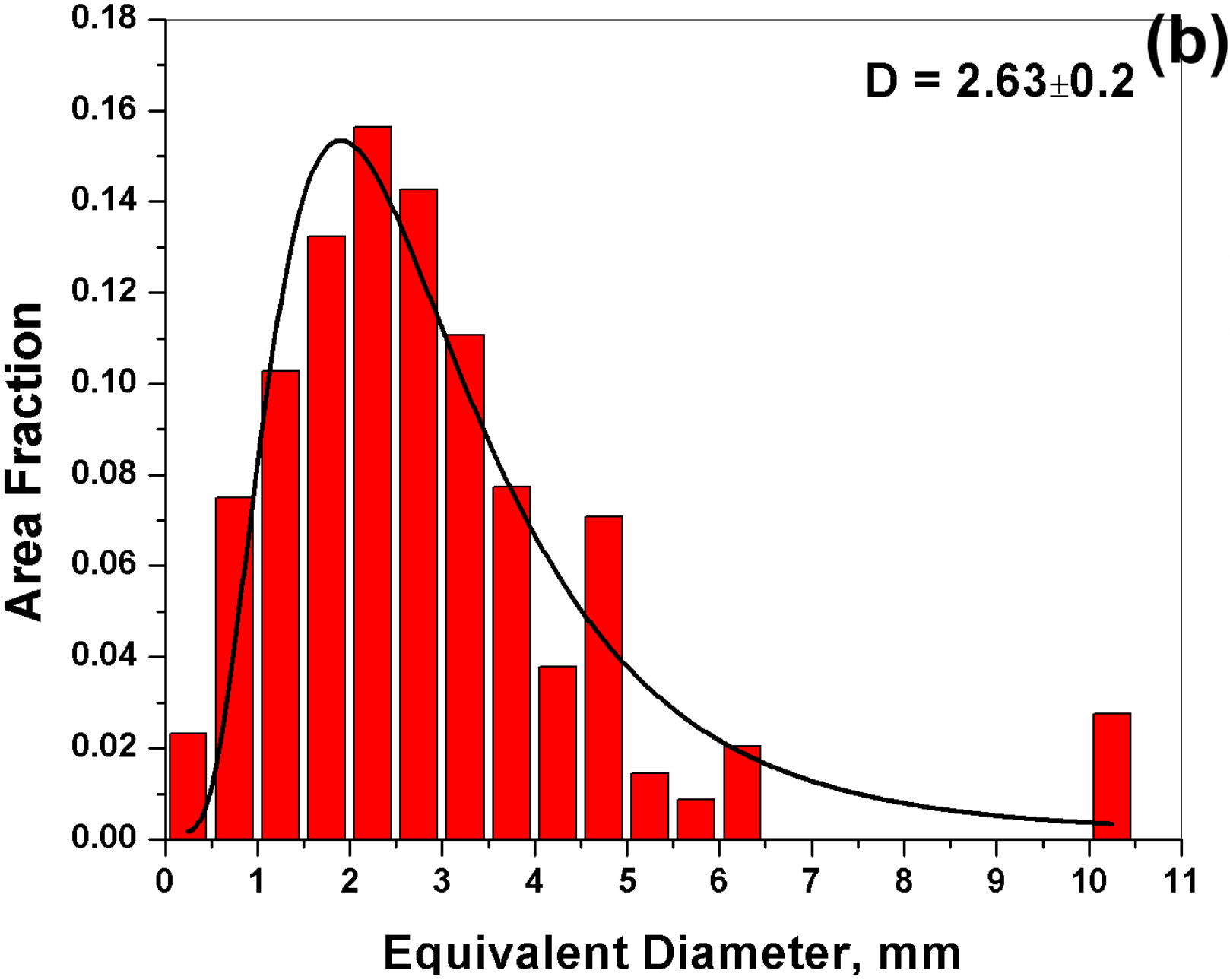
(b)
D = 2.63±0.2
Area Fraction
0.18
0.16
0.14
0.12
0.10
0.08
0.06
0.04
0.02
0.00
0
1
2
3
4
5
6
7
8
9
10
11
Equivalent Diameter, mm

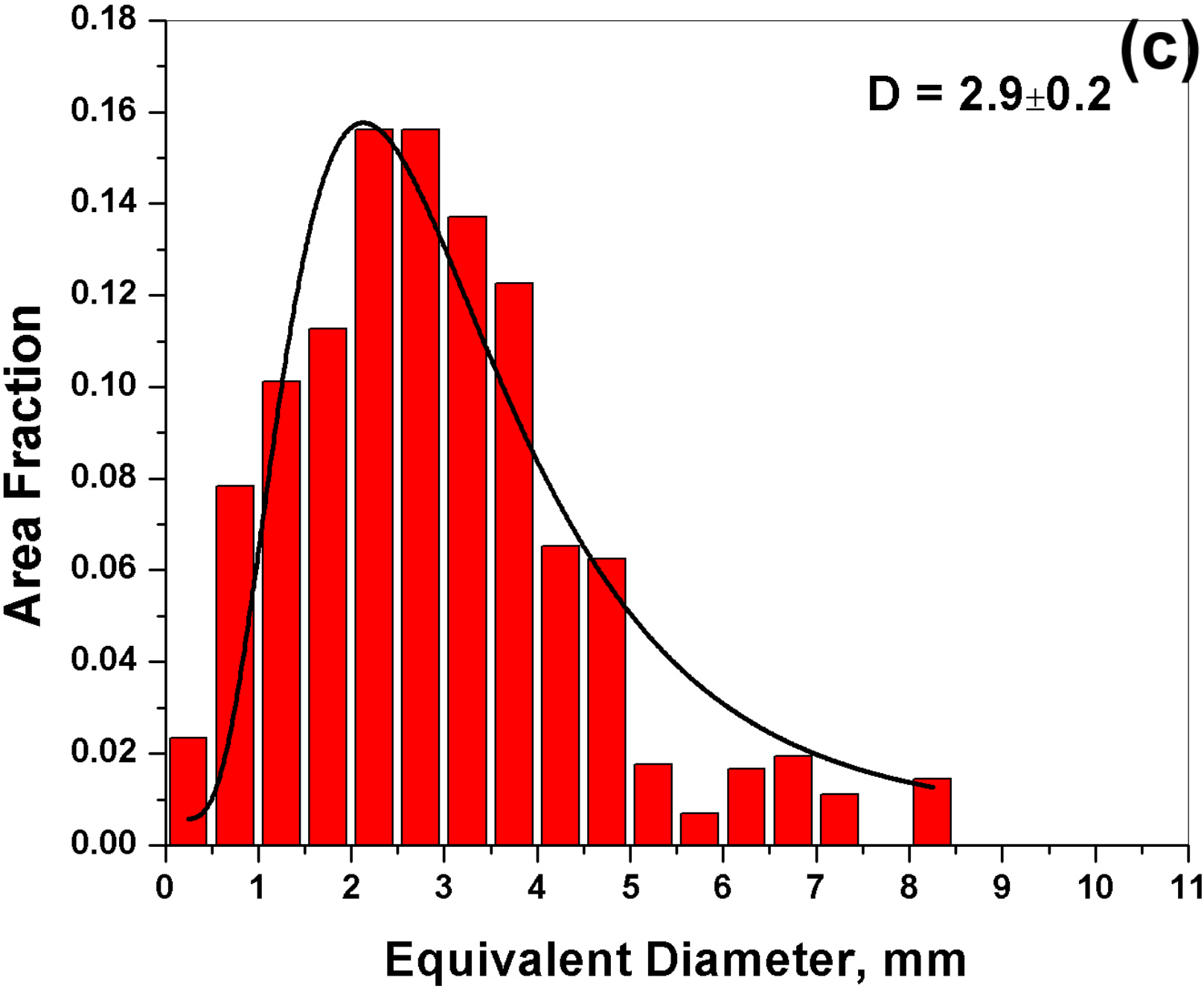
(c)
D = 2.9±0.2
Area Fraction
0.18
0.16
0.14
0.12
0.10
0.08
0.06
0.04
0.02
0.00
0
1
2
3
4
5
6
7
8
9
10
11
Equivalent Diameter, mm

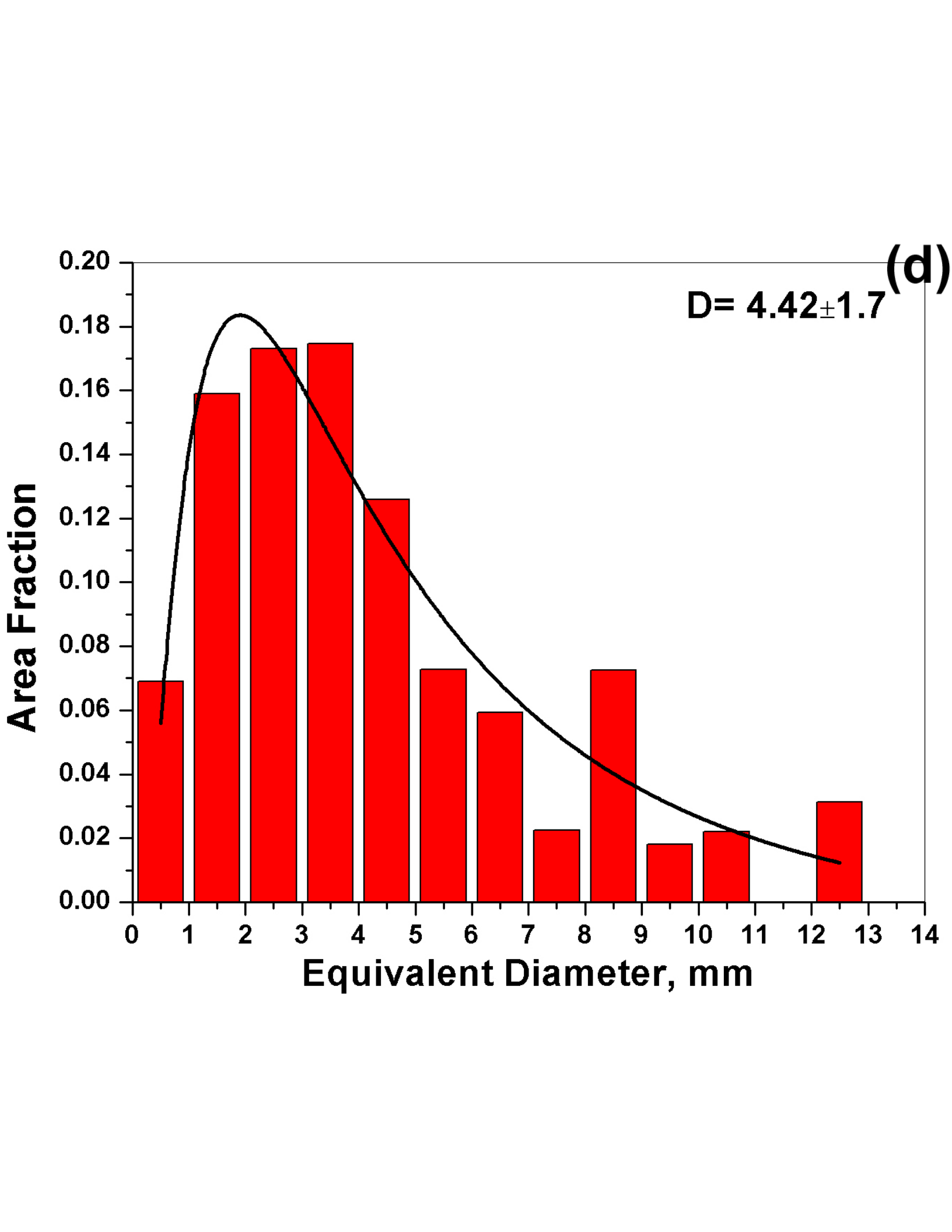
(d)
D= 4.42±1.7
Area Fraction
0.20
0.18
0.16
0.14
0.12
0.10
0.08
0.06
0.04
0.02
0.00
0
1
2
3
4
5
6
7
8
9
10
11
12
13
14
Equivalent Diameter, mm

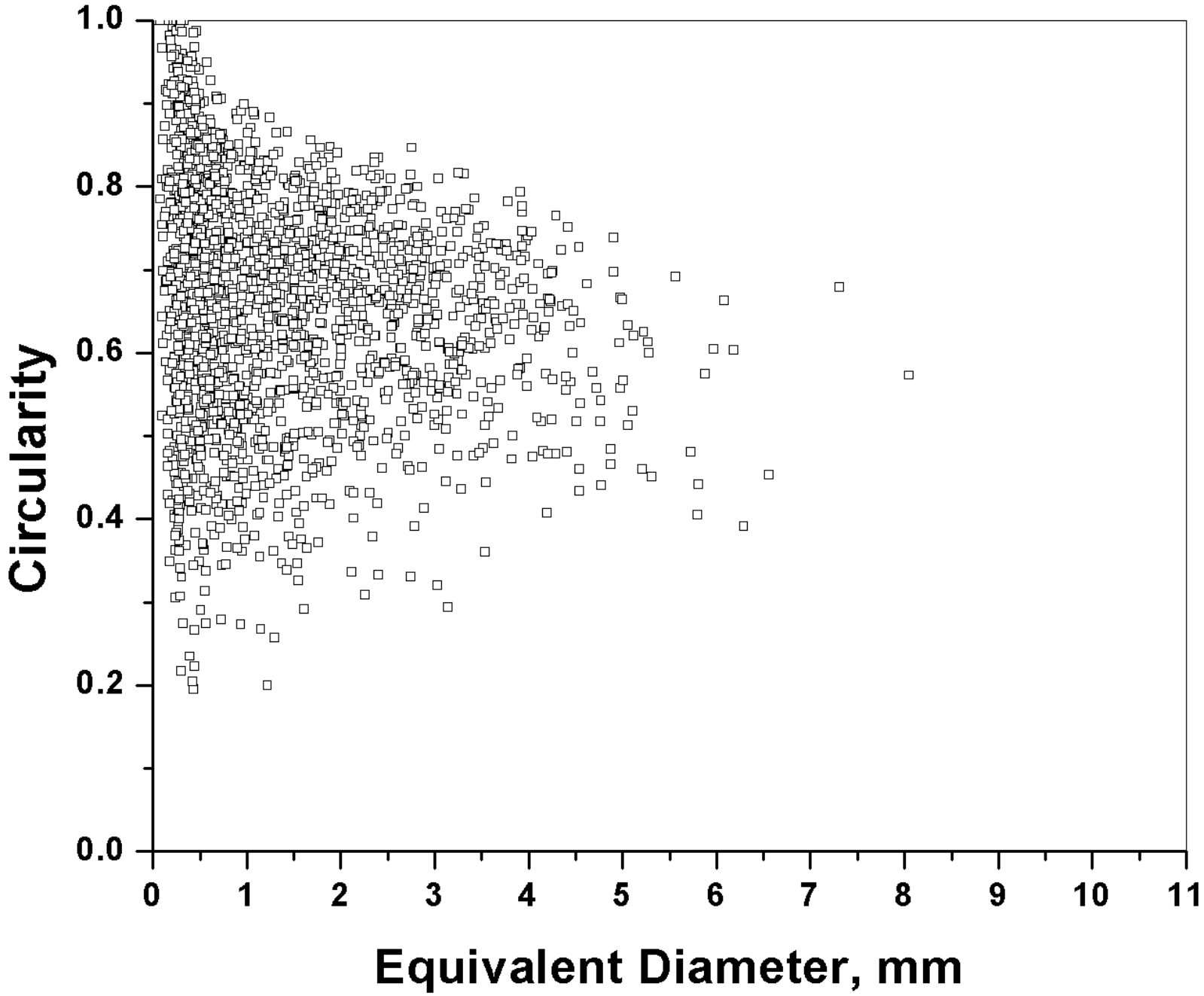
Circularity
1.0
0.8
0.6
0.4
0.2
0.0
0
1
2
3
4
5
6
7
8
9
10
11
Equivalent Diameter, mm

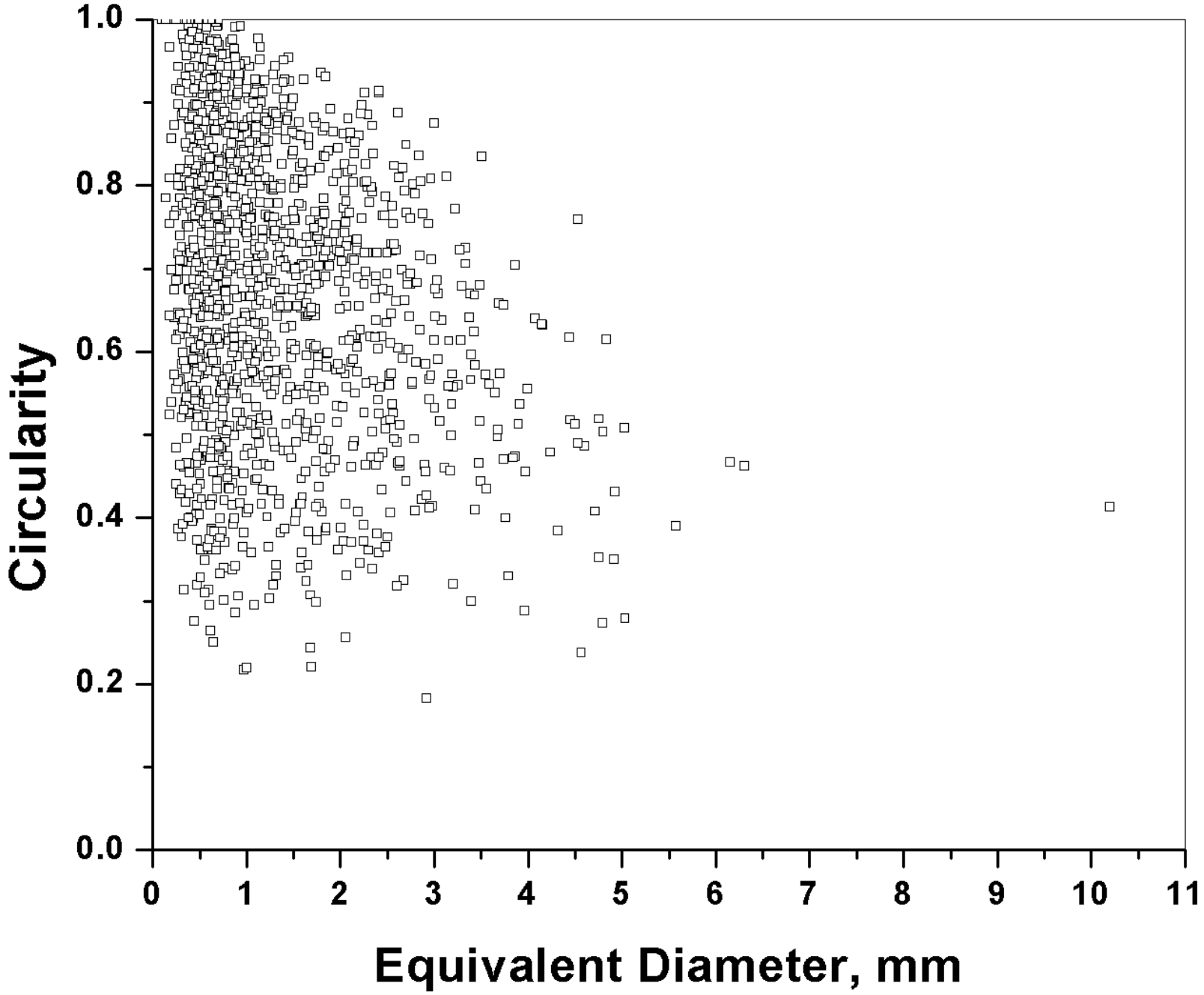
Circularity
1.0
0.8
0.6
0.4
0.2
0.0
0
1
2
3
4
5
6
7
8
9
10
11
Equivalent Diameter, mm

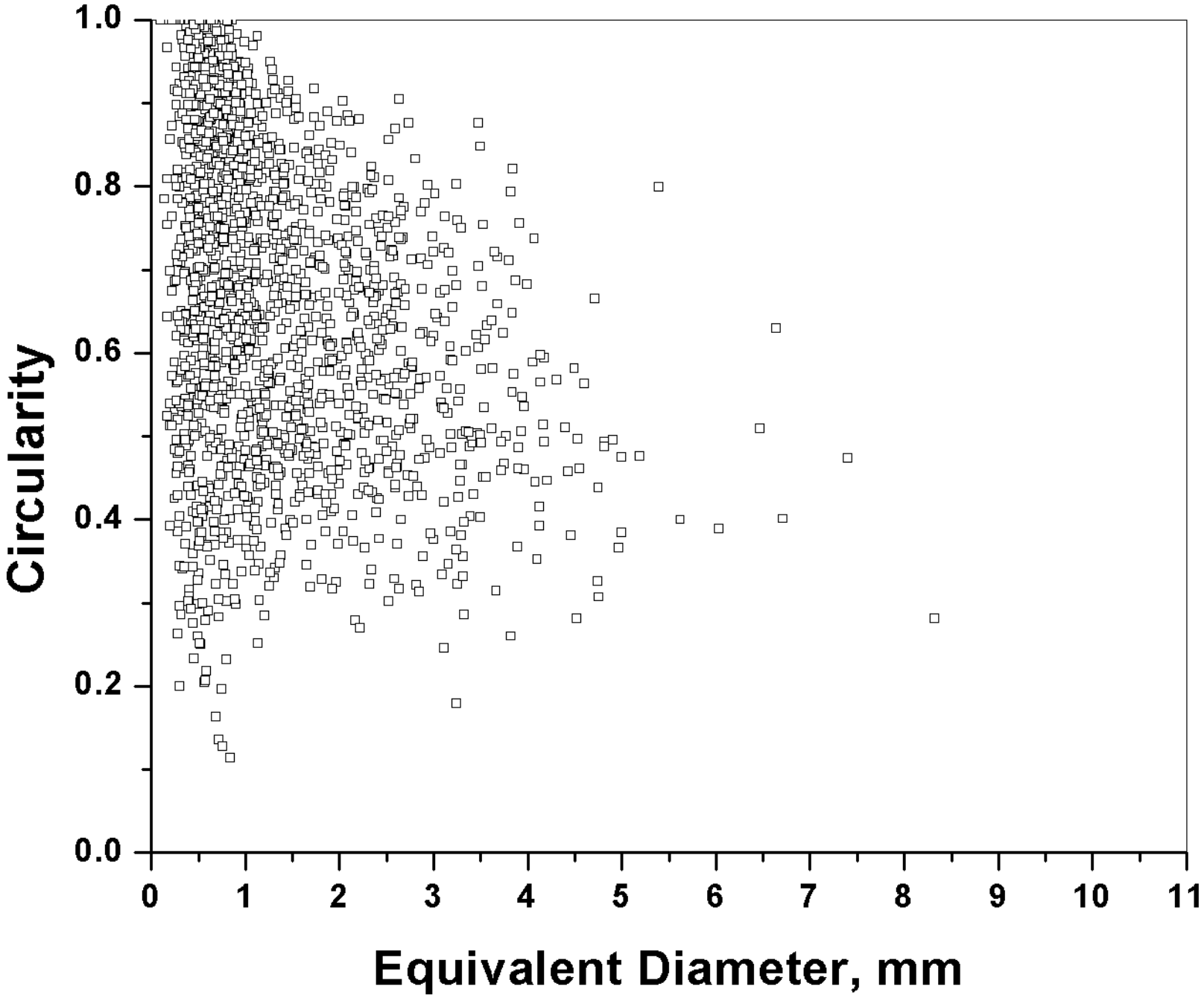
Circularity
1.0
0.8
0.6
0.4
0.2
0.0
0
1
2
3
4
5
6
7
8
9
10
11
Equivalent Diameter, mm

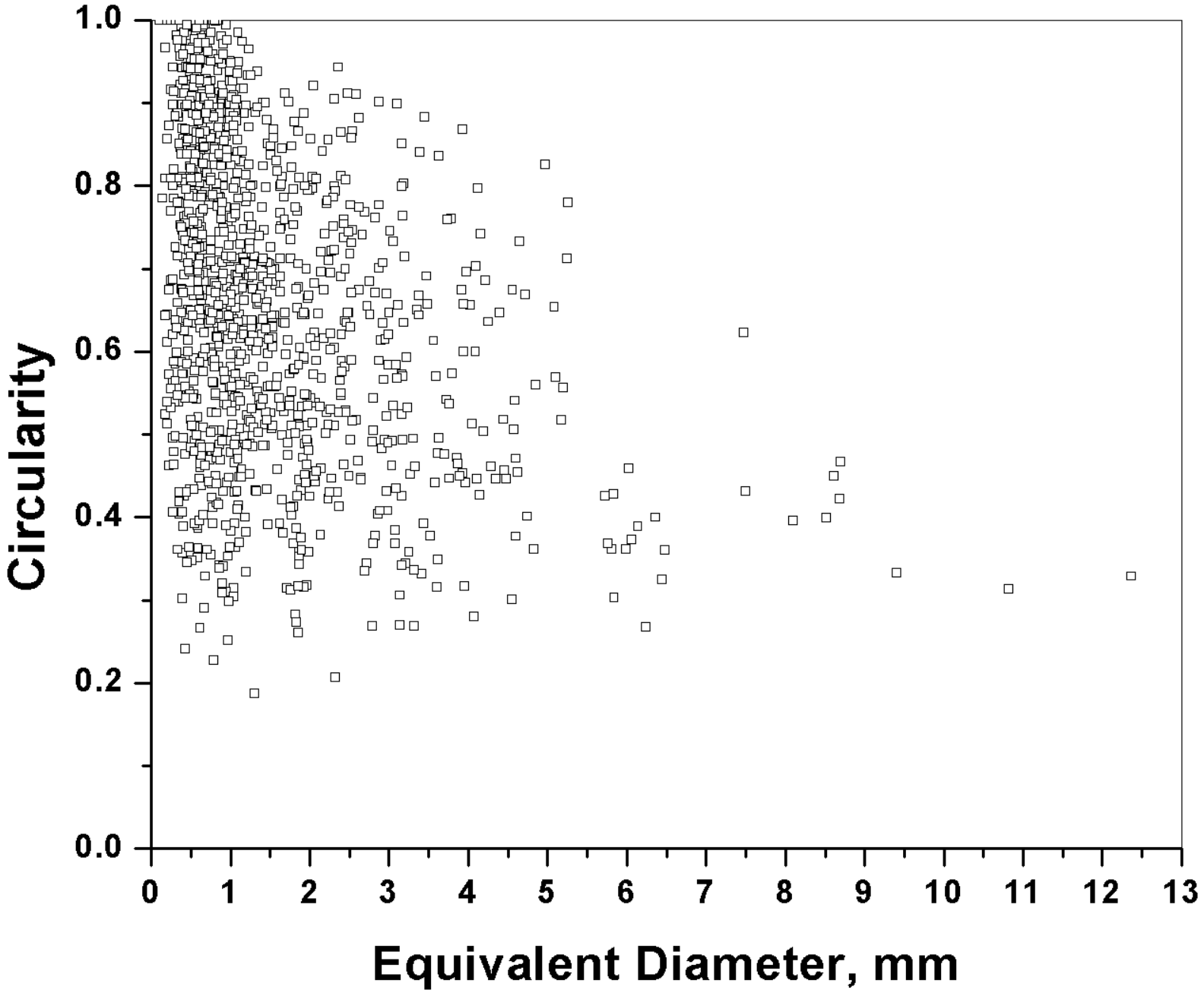
Circularity
1.0
0.8
0.6
0.4
0.2
0.0
0
1
2
3
4
5
6
7
8
9
10
11
12
13
Equivalent Diameter, mm

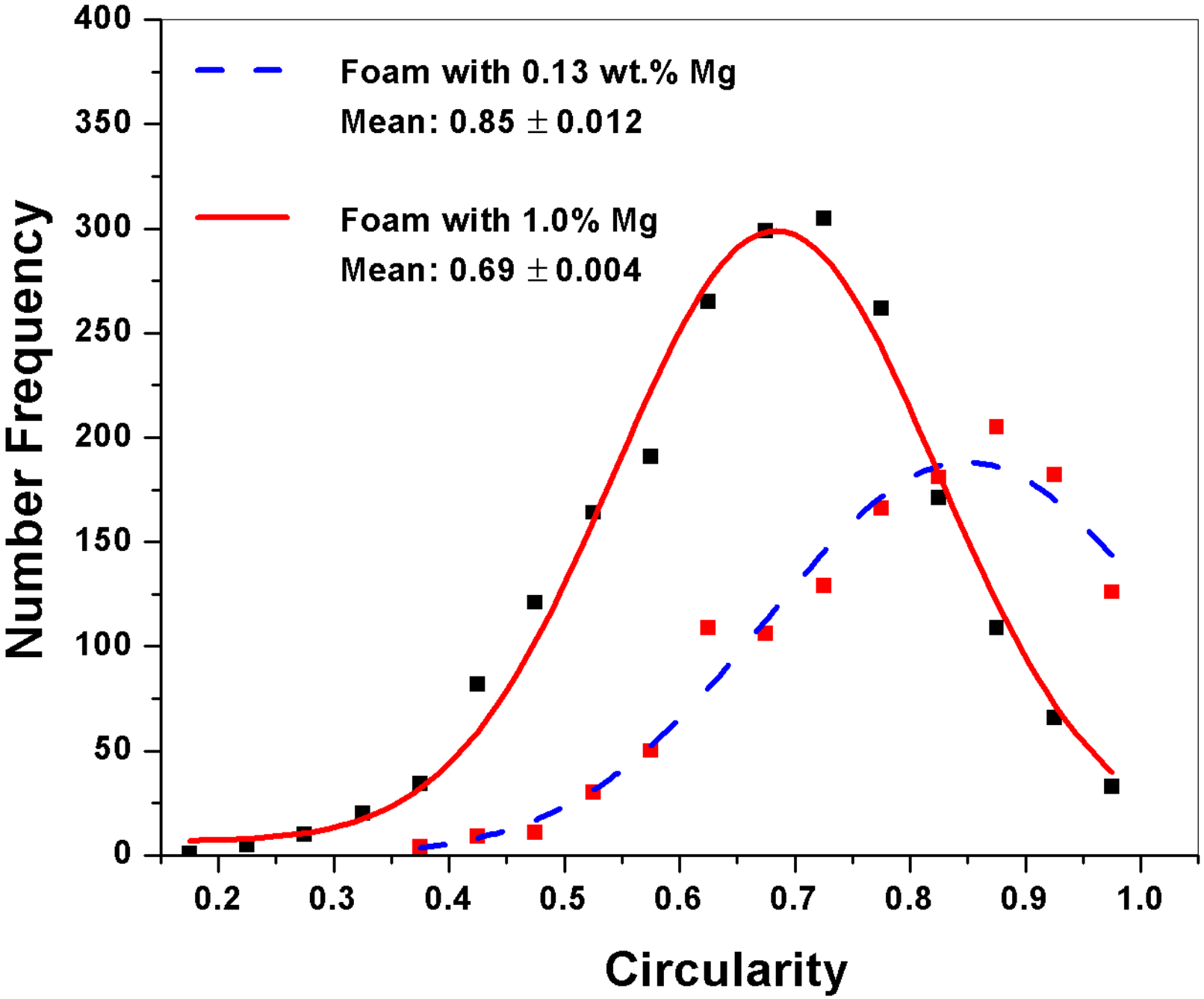
Foam with 0.13 wt.% Mg
Mean: 0.85 ± 0.012
Foam with 1.0% Mg
Mean: 0.69 ± 0.004
Number Frequency
Circularity
400
350
300
250
200
150
100
50
0
0.2
0.3
0.4
0.5
0.6
0.7
0.8
0.9
1.0

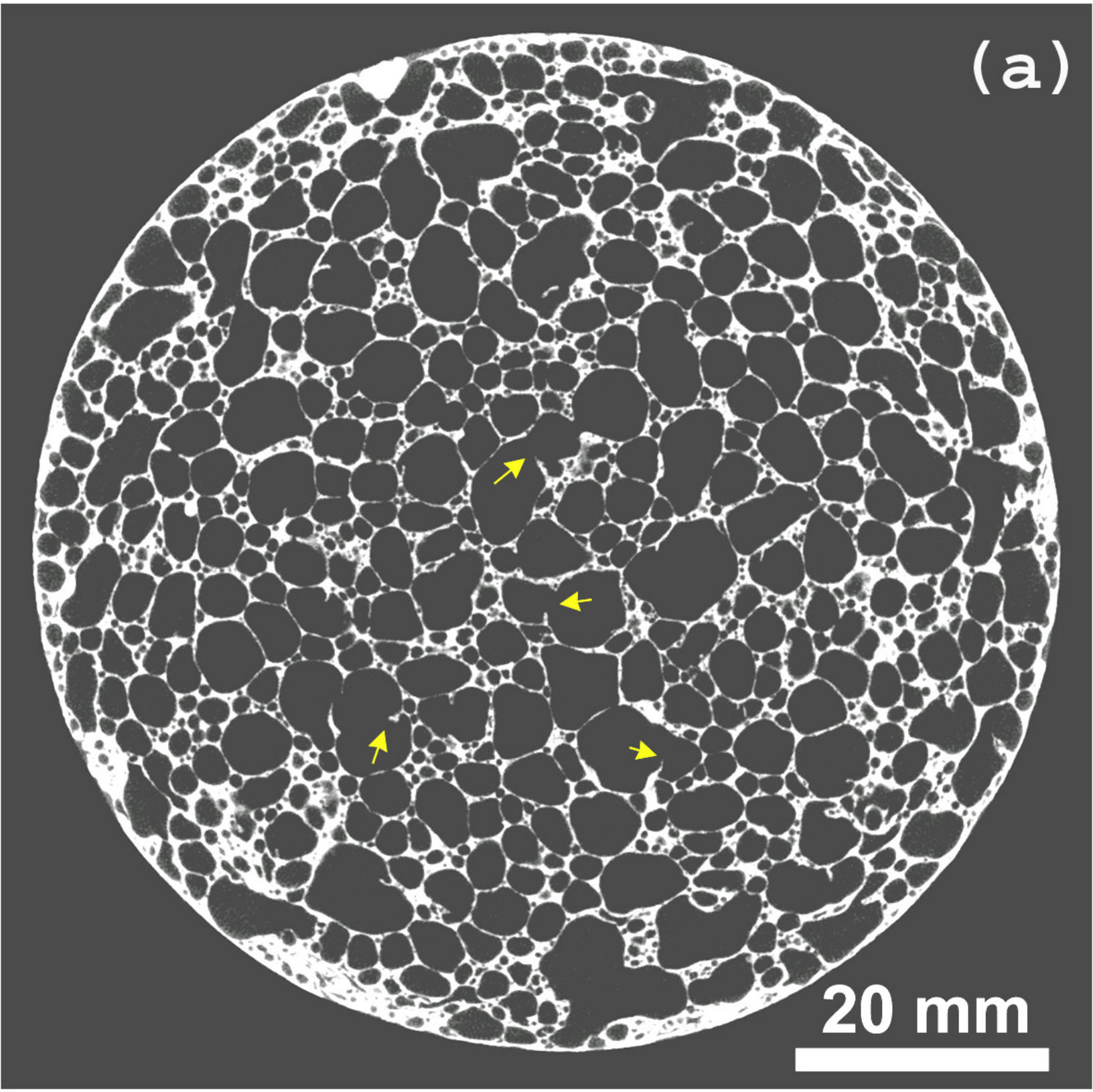
(a)
20 mm

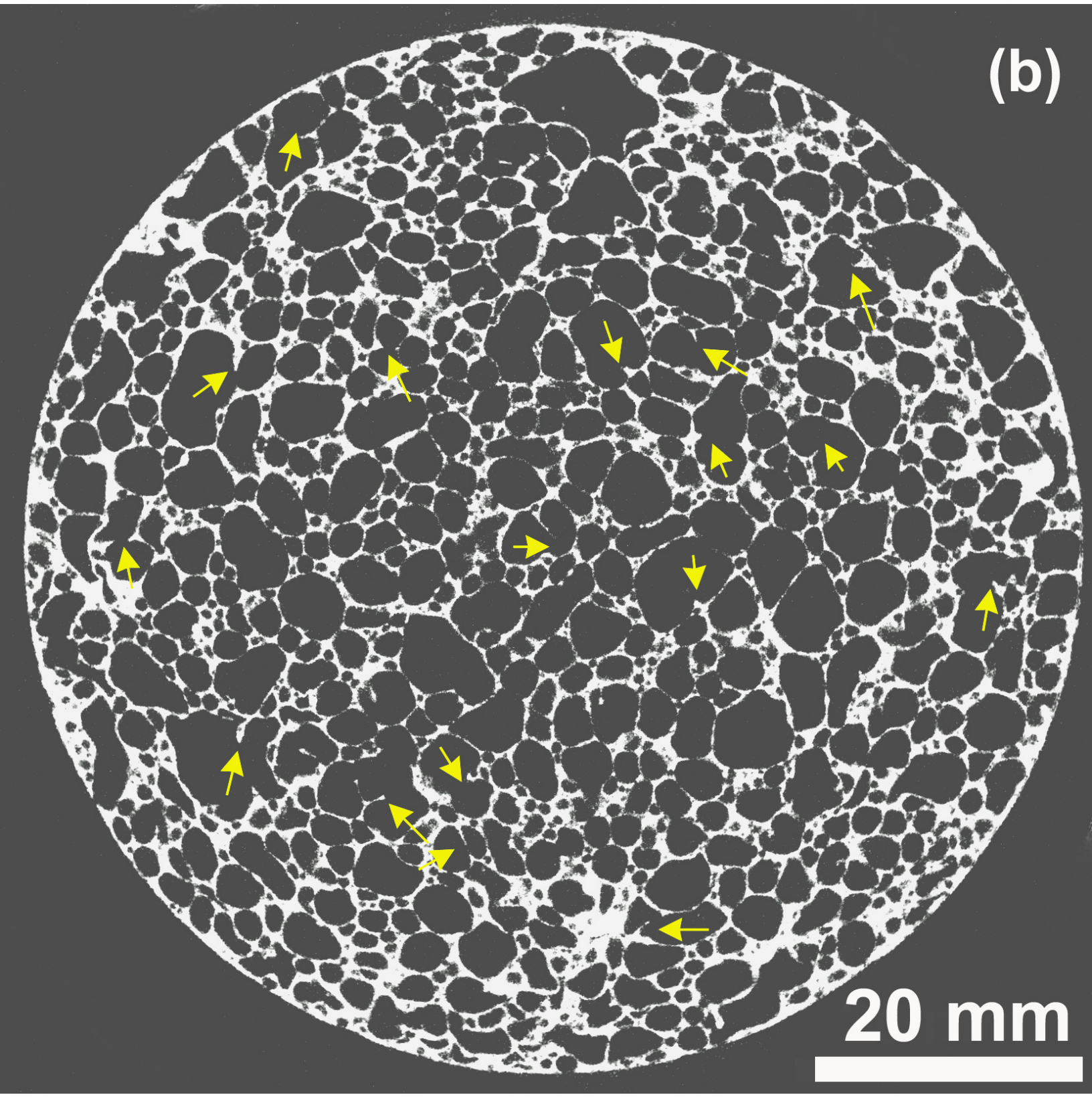
(b)
20 mm

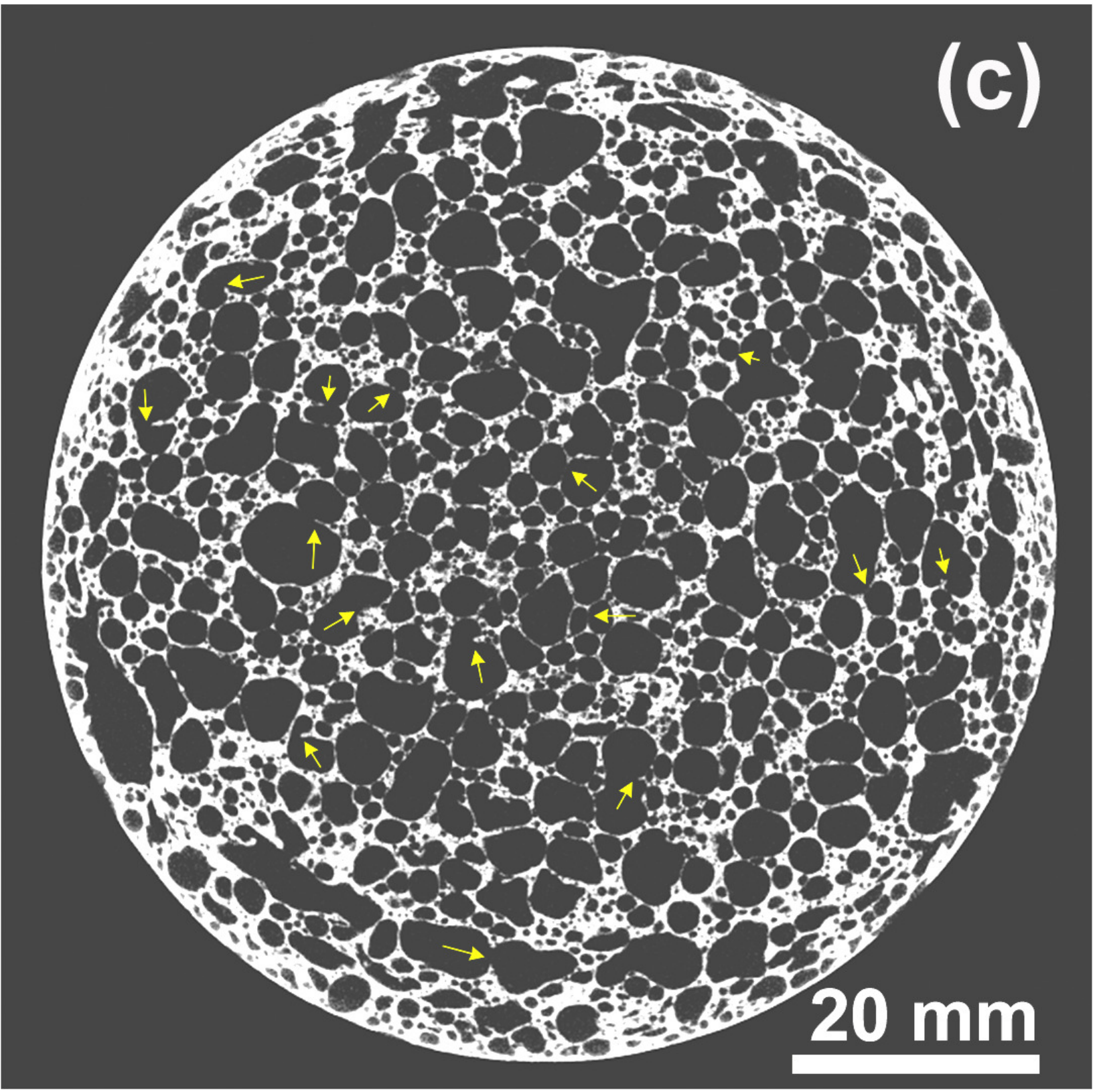
(c)
20 mm

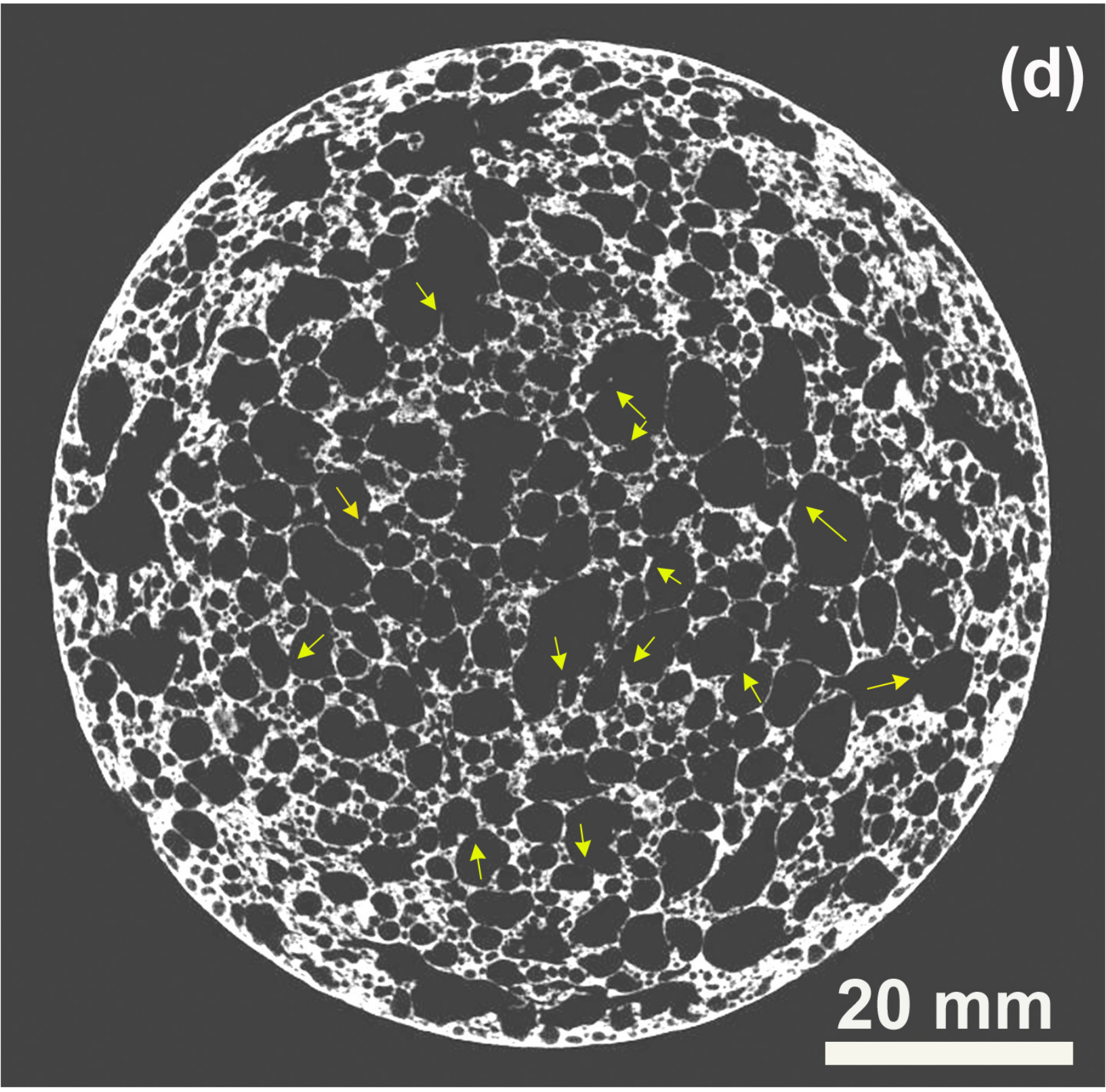
(d)
20 mm

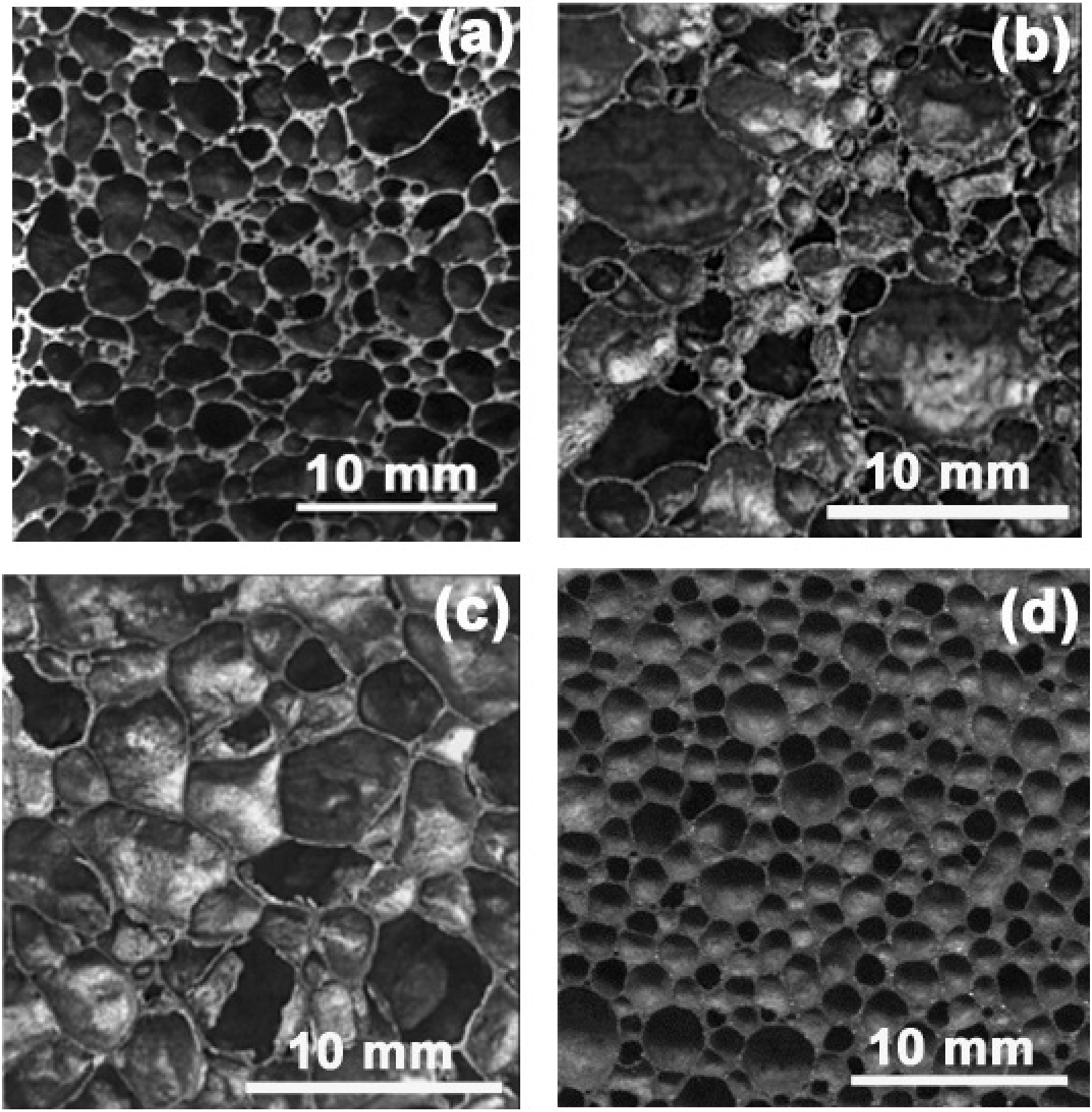
(a)
10 mm
(b)
10 mm
(c)
10 mm
(d)
10 mm

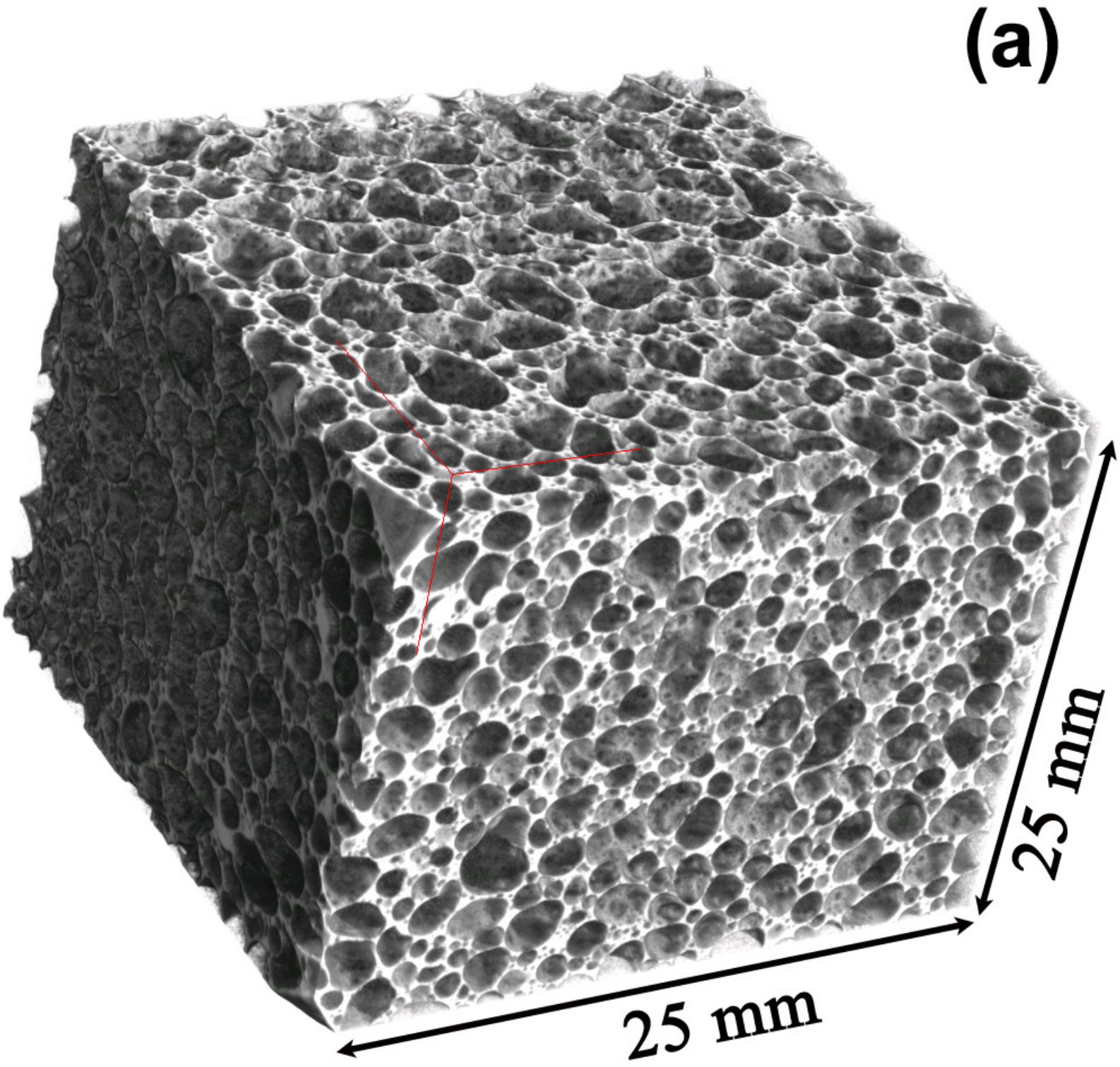
(a)
25 mm
25 mm

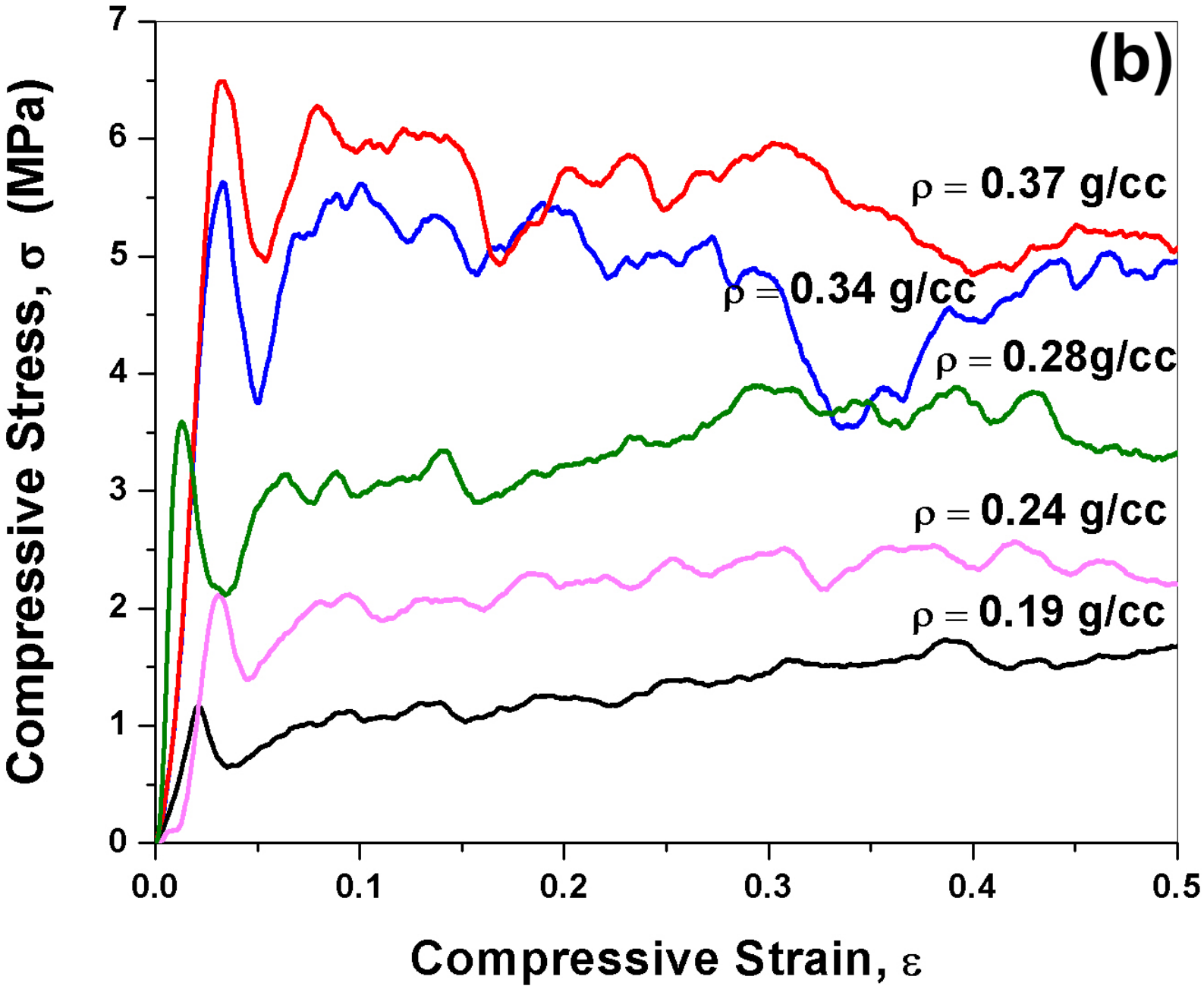
(b)
Compressive Stress, σ (MPa)
Compressive Strain, ε
ρ = 0.37 g/cc
ρ = 0.34 g/cc
ρ = 0.28g/cc
ρ = 0.24 g/cc
ρ = 0.19 g/cc
0
1
2
3
4
5
6
7
0.0
0.1
0.2
0.3
0.4
0.5

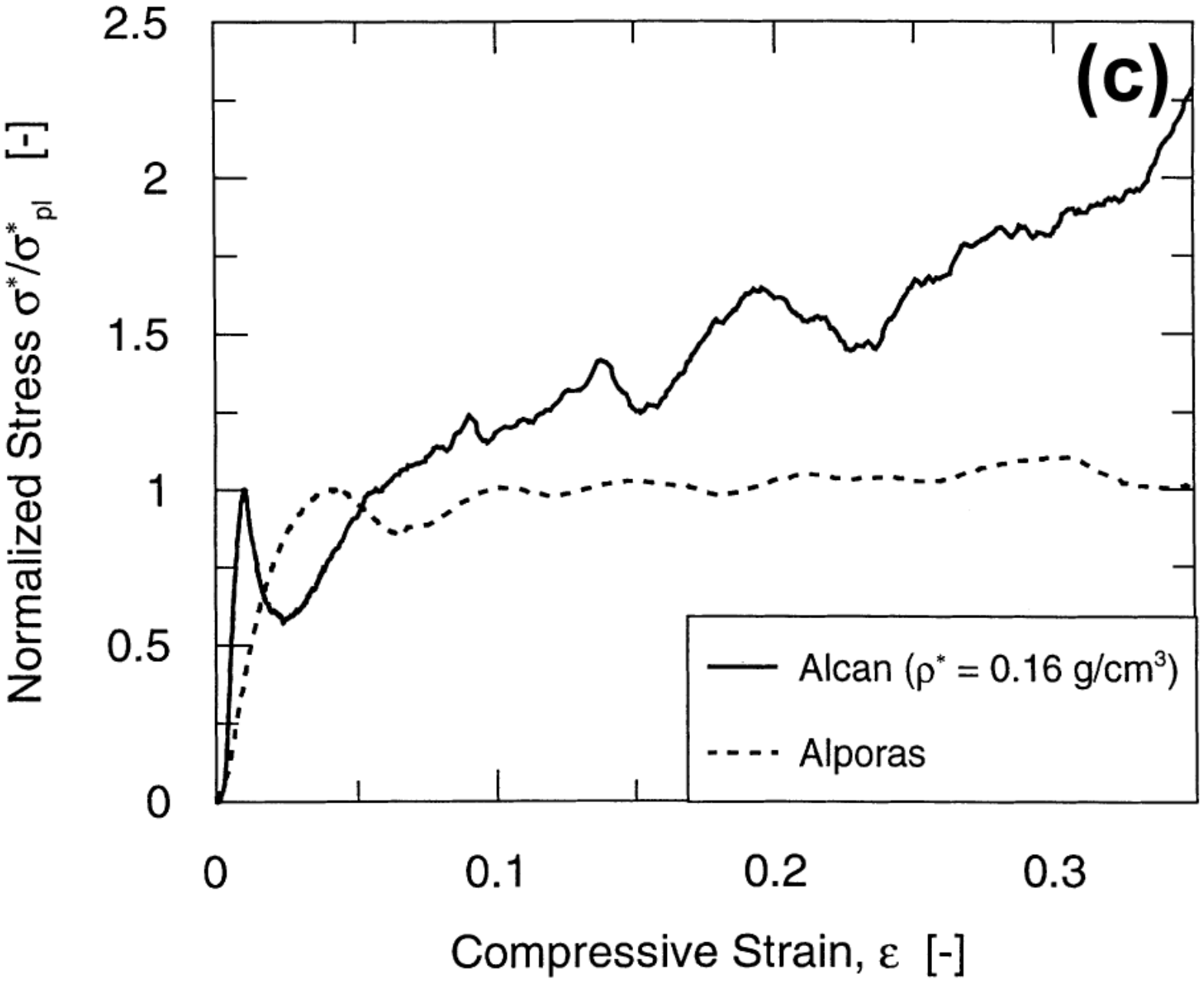
(c)
2.5
2
1.5
1
0.5
0
0
0.1
0.2
0.3
Normalized Stress σ*/σ*pl [-]
Compressive Strain, ε [-]
Alcan (ρ* = 0.16 g/cm3)
Alporas

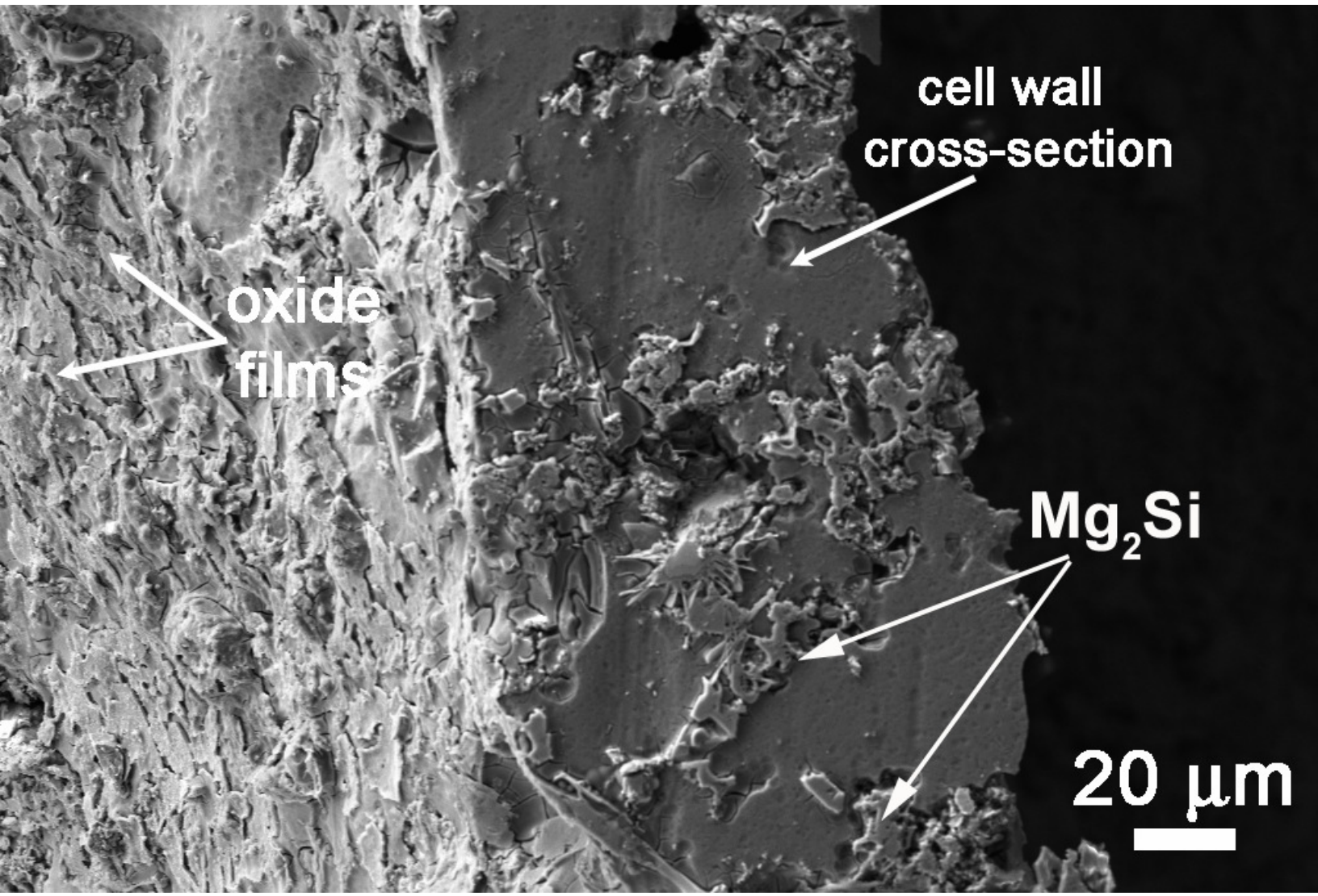
cell wall
cross-section
oxide
films
Mg_2Si
20 µm